

Photovoltaic Generator Modeling for Large Scale Distribution System Studies

A Thesis

Submitted to the Faculty

of

Drexel University

By

Andrew S. Golder

in partial fulfillment of the

requirements for the degree

of

Master of Science in Electrical Engineering

October 2006

© Copyright 2006
Andrew S. Golder. All Rights Reserved.

ACKNOWLEDGEMENTS

I would like to thank my advisor Dr. Karen Miu, for all of her help and guidance in the research and development of this thesis. I also thank her for the opportunity to study and perform research at the Center for Electric Power Engineering (CEPE). My education in the field of power systems engineering began with Dr. Miu as an undergraduate and has continued through my graduate education. I appreciate her skill and enthusiasm as a teacher and mentor; my education here at Drexel University has encompassed much more than the field of power engineering.

I would like to thank Dr. Fischl and Dr. Nwankpa for serving on my thesis committee. Their comments and suggestions throughout the development of this work have been valuable and are greatly appreciated. I appreciate their time and commitment to myself and this work.

TABLE OF CONTENTS

LIST OF TABLES.....	VII
LIST OF FIGURES.....	VIII
ABSTRACT.....	IX
1. INTRODUCTION.....	1
1.1. MOTIVATION.....	1
1.2. BACKGROUND.....	2
1.3. PROBLEM STATEMENT.....	4
1.4. OVERVIEW.....	5
1.5. CONTRIBUTIONS.....	7
1.6. ORGANIZATION OF THESIS.....	7
2. BACKGROUND.....	8
2.1. THE PHOTOVOLTAIC GENERATOR.....	8
2.1.1. THE PHOTOVOLTAIC CELL.....	9
2.1.2. THE PHOTOVOLTAIC MODULE.....	11
2.1.3. THE PHOTOVOLTAIC ARRAY.....	14
2.1.4. THE POWER CONDITIONING UNIT.....	14
2.1.4.1. THE MAXIMUM POWER POINT TRACKER.....	15
2.1.4.2. THE DC TO AC INVERTER.....	16
2.2. UNBALANCED DISTRIBUTION POWER FLOW.....	18
2.2.1. CONSTANT PQ SOURCES.....	20
2.2.2. CONSTANT P V SOURCES.....	21

3. PHOTOVOLTAIC ARRAY MODEL.....	24
3.1. CHARACTERISTIC EQUATION OF THE NON-IDEAL PHOTOVOLTAIC CELL.....	26
3.2. CONVERSION OF CELL CHARACTERISTIC EQUATION TO ARRAY CHARACTERISTIC EQUATION	28
3.3. STEP BY STEP MODELING PROCEDURE.....	31
3.3.1. DETERMINE THE CONNECTION SCHEME OF THE ARRAY.....	31
3.3.2. CONVERT CELL CHARACTERISTIC EQUATION TO ARRAY CHARACTERISTIC EQUATION.....	33
3.3.3. SOLVE FOR PARAMETERS OF CHARACTERISTIC ARRAY EQUATION.....	34
3.3.4. CALCULATE THE I-V CURVE OF THE CHARACTERISTIC EQUATION AND DETERMINE P_G^{DC}	39
3.4. FLOW DIAGRAM OF PROCEDURE FOR CALCULATING POWER OUTPUT OF PHV ARRAY.....	42
3.5. IMPLEMENTATION AND EXAMPLE.....	43
4. MODEL OF THE POWER CONDITIONING UNIT AND INTEGRATION WITH POWER FLOW.....	45
4.1. POWER CONDITIONING UNIT MODELING.....	46
4.1.1. THE CONSTANT PQ SOURCE MODEL.....	46
4.1.2. THE CONSTANT P V SOURCE MODEL.....	47
4.2. POWER FLOW INTEGRATION.....	48

4.2.1. PQ SOURCE MODEL INTEGRATION.....	49
4.2.2. P V SOURCE MODEL INTEGRATION.....	49
5. SIMULATION METHODS AND RESULTS.....	51
5.1. TEST SYSTEM AND CASE FILE CONSTRUCTION.....	51
5.1.1. ELECTRICAL SYSTEM DATA.....	52
5.1.2. ENVIRONMENTAL DATA.....	53
5.2. SINGLE FLOW STUDIES.....	54
5.3. TWENTY FOUR HOUR SIMULATION STUDIES.....	55
5.3.1. EXAMPLE TWENTY FOUR HOUR SIMULATION STUDY....	56
5.3.2. OBSERVATIONS AND REMARKS.....	59
6. CONCLUSION AND FUTURE WORK.....	61
6.1 CONCLUSIONS.....	61
6.2. SUMMARY OF RESEARCH CONTRIBUTIONS.....	62
6.3. FUTURE WORK.....	63
LIST OF REFERENCES.....	65
APPENDIX A: List of Symbols by Section.....	69
APPENDIX B: Derivation of V_{ocAE}	73
APPENDIX C: CALCULATING THE LOAD LEVEL FOR A GIVEN POWER FLOW	75
APPENDIX D: EXAMPLE SOLAR MODULE SPEC SHEET	78

LIST OF TABLES

Table 5.1: Summary of simulation study conditions.....	51
Table 5.2: Imbalance study varying PHV penetration.....	55

LIST OF FIGURES

Figure 2.1: Typical connection scheme of a residential or commercial PHV generator....	8
Figure 2.2: Circuit model of an ideal solar cell.....	10
Figure 2.3: String of cells with bypass and blocking diodes.....	12
Figure 2.4: Components of the power conditioning unit.....	15
Figure 2.5: I-V Characteristic of a solar module under varied solar irradiance.....	16
Figure 2.6: I-V Characteristic of a solar module under varied ambient temperature.....	16
Figure 2.7: The basic building block of a distribution system.....	19
Figure 3.1: I-V curve showing the three points given on a typical specification sheet...	25
Figure 3.2: Electrical model of a solar cell with shunt resistance.....	26
Figure 3.3: Model of a solar cell without shunt resistance.....	28
Figure 3.4: Circuit diagram of a 3x3 solar array.....	29
Figure 3.5: Flow diagram of PHV array model.....	42
Figure 3.6: I-V Characteristic of example PHV Array.....	43
Figure 3.7: P-V Characteristic of example PHV Array.....	44
Figure 5.1: One line diagram of 394 bus test system.....	52
Figure 5.2: Real power demand of the 394 bus test case for peak load.....	57
Figure 5.3: TMY2 Irradiance profile for Binghamton NY, July 16.....	58
Figure 5.4: TMY2 Ambient temperature profile for Binghamton NY, July 16.....	58
Figure 5.5: Real power demand at the substation under varying capacity of PHV generation.....	59
Figure 5.7: Real power output of a 1000W rated PHV generator.....	60

ABSTRACT

Photovoltaic Generator Modeling for Large Scale Distribution System Studies

Andrew S. Golder

Dr. Karen Miu, Ph.D.

Geographic regions with favorable conditions for photovoltaic (PHV) power generation are seeing increasing numbers of three-phase commercial installations and single-phase residential sized installations. PHV sources can be described as intermittent sources because their power production is a function of ever changing environmental conditions. Increased numbers of these intermittent sources will begin to have a significant impact on the distribution system. This work presents the development of a simulation model for utility distribution systems with installed PHV generation. The mathematical modeling of PHV generators is investigated and a model is developed to calculate power output based on the environmental conditions which determine generator behavior. This output is then integrated into an unbalanced distribution power flow solver using either a constant PQ or constant P|V| generator model. The model has been implemented and simulations will be presented for a 394 bus test system. In order to accommodate intermittency, hourly simulations which utilize corresponding environmental conditions and 24 hour load curves have been automated. Simulations are performed in order to perform system studies in the areas of demand profiles, phase balancing, feeder balancing, power factor changes and voltage rise. Analysis is performed to identify issues that will be most relevant to engineers working in planning and operations of distribution systems with installed PHV generation.

1. Introduction

1.1 Motivation

Photovoltaic (PHV) power generation has an increasing importance in the renewable energy marketplace due to its ability to quietly produce emission free power at the load site. The main advantage of these systems over other forms of renewable energy is the feasibility of small PHV systems which can be owned and operated by the consumer. Economic and political trends, along with increased social desire for alternative energy sources has produced a significant increase in the installation of small scale (on the order of 1kW) residential and commercial PHV power systems on the utility distribution system. In the US, as of 2003, 15 states have implemented programs which encourage or mandate the growth of renewable energy [9]. In addition some utilities such as Austin Energy of Texas, USA have offered their customers rebates up to \$4.00 per watt to help offset the installation cost of PHV systems [2]. In 2006 the California state government passed the California Solar Initiative (CSI) which is the largest solar energy policy enacted in the US. The initiative allots \$2.9 billion dollars for solar energy rebates which will aid residents and businesses in reducing the installation costs of PHV generation systems. The goal of the CSI is to increase installed solar capacity in California by roughly 3000 MW over an 11 year span from 2006-2017 [4].

While PHV generation is not a new technology, the socio-economic factors described above are currently causing a significant and rapid increase in the total installed capacity of grid connected PHV generation in the United States. Because PHV generation is most often owned and operated by the consumer, system planners and operators have reduced knowledge of and control over the distribution systems yet it is

their responsibility to manage these networks. This situation is similar to system loads where the day to day behavior of which is determined by the customer. However in the case of loads the utility has more control over where new loads are connected to the existing network, where as the location and sizing of PHV generators is determined by the customer. As installed capacity increases, planners and operators will be faced with an entirely new set of problems and challenges which will require new engineering solutions.

When developing engineering solutions a basic tool used to predict system behavior, identify problems which are most likely to occur, and test the optimal control schemes is power flow analysis. Power flow analysis requires mathematical models of every component connected to the power system being studied. Thus it is important to develop models which allow for distribution system analysis with PHV generation to be performed.

1.2 Background

PHV generators are most often connected to the distribution system for several reasons. A high percentage of grid connected PHV generators are owned by small, residential and commercial consumers, and are therefore connected at the load site on the distribution system. When compared to other forms of distributed generation, PHV generators are typically physically small, low voltage, and low power systems and it is therefore appropriate to interface these systems with the low voltage distribution system. PHV generation is unique in that the residential and small commercial systems for example in the U.S. which make up a majority of the installations are often configured for single phase power generation. It is therefore appropriate to connect PHV generators

to the distribution grid which contains single phase feeders and is designed to handle an unbalanced flow of power.

The study of renewable generation in utility distribution systems began in the late 1970's. Procedures for evaluating the impact of intermittent generation on distribution system planning and operations were presented in [17, 18]. Subsequent studies have compared power demand curves with PHV production curves in order to predict system load profiles [12]. Other studies have calculated line loss savings from a distribution PHV system installation based on simplified distribution line models [13]. To this date an unbalanced distribution power flow solver incorporating PHV generation has not been developed and documented publicly. While PHV generation systems have been in use since the late 1970's economic considerations have limited their contribution to overall power production, and the distribution power system impacts of these small number of installations has not seen extensive study. In addition unbalanced distribution system modeling and power flow analysis, which increase the accuracy of distribution system analysis were developed in the late 80's and 90's and have only recently evolved as state of the art methods [35, 36]. Recently in the early 21st century economic and political trends suggest that certain geographic areas could see high penetrations of PHV generation on the distribution system, and therefore studies of their impact on large scale distribution systems are warranted.

The characteristics of utility distribution networks provide engineers with a unique set of problems. For example in order to counteract the inherently unbalanced nature of distribution systems load balancing schemes have been investigated and have been implemented typically in seasonal manners [3, 1] and more recently with higher

frequency [8]. Methods to enhance the voltage stability and reduce power losses of distribution systems by optimal placement and control switching of capacitors have been investigated in [23, 32]. Schemes for service restoration of distribution systems have been investigated in [22, 24, 25] utilizing techniques including network configuration and capacitor control. Investigations in the field of distribution automation are extensive with goals such as cost reduction [34], reliability improvement [28], and power quality monitoring [19].

Now, with a significant number of small scale, single-phase PHV systems coming online, it may be useful to make updates to these works in order to include the special case of distribution systems with significant capacity of installed PHV generation. In addition, the intermittent nature of PHV generation creates new challenges with regard to distribution capacity planning and maintaining load balance. New distribution system analysis and automation tools are needed to accommodate the problems associated with grid connected PHV generation.

1.3 Problem Statement

The objective of this work is to develop a component model for grid connected PHV generation which can be integrated with an unbalanced distribution power flow solver. The component model must be practical for use by system planners and operators in order to serve its function for systems level studies. Then, a combined model, which describes the PHV generator and system models together, will use state of the art methods and equations for PHV generator modeling and unbalanced distribution power flow. The model will be implemented using an existing unbalanced distribution power flow solver coded in MATLAB in order perform simulation studies.

1.4 Overview

This work presents the development of a system model which simulates distribution systems with grid connected photovoltaic generation. The model is formed by the integration of *i*) a mathematical component model of a photovoltaic (PHV) generation system, with *ii*) an existing unbalanced distribution power flow solver. A simulation tool has been developed using MATLAB which is used to simulate the behavior of distribution systems with grid connected PHV generation over the course of a day.

The mathematical model of the photovoltaic generator is composed of two parts which model the two main components of the PHV generator, the photovoltaic array, and the power conditioning unit (PCU). First the model of the PHV array calculates the DC power output under the given environmental conditions. Second the model of the PCU converts the DC power value to a specific AC power injection to the utility grid. These two models are now discussed respectively.

The basic building block of the PHV array model is the standard equation which describes the I-V characteristic of a single solar cell. By making some assumptions it is possible to perform scaling operations in order to define an equation which describes the I-V characteristic of a PHV array. The developed model uses the available inputs to calculate the required parameters of the array characteristic equation. Because the solution to the characteristic equation is not unique an appropriate initial condition and iterative technique are used to calculate the solution vector of the array characteristic equation. The model then determines the solution corresponding to the maximum power output, and defines this as the DC power output of the PHV array.

The model of the PCU is characterized by the choice of one of two inverter control schemes, which determines the use of either a constant PQ injection or a constant P|V| injection model. In both schemes the DC power output of the PHV array is first scaled down according to the efficiency of the PCU, and second an AC power injection to the distribution system is calculated.

A previously developed unbalanced distribution power flow method provides the steady state model of the utility distribution system. A traditional Newton Raphson method is used to perform three phase power flow analysis using the appropriate component models for unbalanced distribution power flow. Power injections determined by the PHV array model are integrated with the power flow using the traditional PQ and P|V| generator models. The overall model of the power system is used to perform power flow analysis in order to model the steady state behavior of the distribution system. Therefore the model is an instantaneous model which describes the steady state behavior of the power system at a single point in time.

The model of a distribution system with PHV generation is implemented in MATLAB and simulations are performed using a 394 bus test system. Twenty four simulations, each of which represents the average behavior of the system for the time period of one hour, are used to study the system conditions over the course of the day. Profiles for load demand and environmental conditions are used to simulate the test system for varying seasonal, environmental, and loading conditions. Analysis is performed with a primary focus placed on phase balancing and feeder balancing. Several issues are addressed with the goal of identifying the problems which are most relevant to distribution system planners and operators.

The following sections describe the characteristics of PHV generators which make it appropriate for them to be connected to the utility distribution system. It then details the background and history of distribution systems studies involving PHV generation. Literature regarding distribution systems which may be impacted by the installation of grid connected PHV generation is also discussed.

1.5 Contributions:

The following contributions are presented in this thesis:

- Practical PHV generator model for systems engineers requiring limited input data
- Matlab based simulation tool which integrates the PHV model with an unbalanced distribution power flow solver for system studies
- Simulation methods, results, and analysis for 24 hour system studies using a 394 bus test case.

This thesis provides an additional component model for the field of steady state distribution power system analysis.

1.6 Organization of Thesis

Chapter 2 is a review of *i)* PHV generators, their components and functions, and *ii)* unbalanced distribution power flow and PQ and P|V| generator models. Chapter 3 describes the PHV array model, specifying all input and output parameters, assumptions and procedures. In Chapter 4 the PCU model and integration of the calculated power injection with unbalanced distribution power flow analysis is described. Chapter 5 presents simulation methods, procedures, results, and analysis. In Chapter 6 some conclusions are made.

2. Background

This chapter reviews two subjects important to modeling installed PHV generation on a distribution system:

- First, a grid tied photovoltaic generator, its components and their functions.
- Second, unbalanced distribution power flow methods with a focus on co-generator modeling.

2.1. The Photovoltaic Generator

A photovoltaic generator is a device which converts energy in the form of solar radiation to energy in the form of electric current. The basic component of a PHV system is the photovoltaic cell. Multiple cells are connected in series and parallel to form solar panels or modules, which are sold commercially for applications such as grid tied solar generation. Solar modules are connected in series and parallel in order to create a PHV array. The solar array produces DC power which for grid tie systems must be adjusted by a maximum power point tracker (MPPT) and then converted to AC by a DC to AC inverter. These functions are performed by the power conditioning unit (PCU) which is composed of the MPPT and inverter [29]. An example a PHV generator system without energy storage devices is shown in Figure 2.1. In the discussion below the PHV array and its components will be addressed first followed by the PCU and its components.

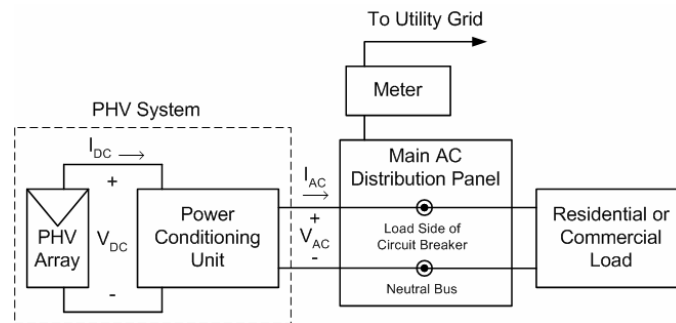


Figure 2.1: Typical connection scheme of a residential or commercial PHV generator

2.1.1. The Photovoltaic Cell

The photovoltaic cell is a semiconductor device which behaves as a current source when driven by a flux of solar radiation from the sun. This occurs when radiation is incident upon absorbing material and separates positive and negative charge carriers in the presence of an electric field. The electric field exists permanently at junctions or inhomogeneities in solar cells which can be described as silicon semiconductor junction devices. A silicon semiconductor junction device contains a p-n junction similar to that of a common diode, however in a solar cell it exists over a large surface area. When not illuminated and connected to a forward bias the ideal solar cell mimics the electrical characteristics of an ideal diode, modeled by the Shockley equation (2.1), where the current produced is referred to as the dark current I_D :

$$I_D = I_o \left(e^{\frac{V_c q}{k T_{cK}}} - 1 \right) \quad (2.1)$$

where:

I_D = dark current (A)

I_o = saturation current of the diode (A)

V_c = cell voltage (V)

$q = 1.6 * 10^{-19}$ (coul)

$k = 1.38 * 10^{-23}$ (j / K)

T_{cK} = Cell Temperature (K)

The current in the cell that results from solar radiation is called the photo current I_l which flows in the direction opposite of the forward dark current. Its value remains the same regardless of external voltage and therefore it can be measured by the short circuit current ($I_{sc} = I_l$). This current varies linearly with the intensity of solar radiation as

increased radiation is able to separate increased charge carriers. The overall current is then described as the difference between the dark current and the photocurrent. If the sign convention of current flow is reversed to describe the current which is produced by an illuminated cell (I_c) then the cell equation can be written as shown in (2.2):

$$I_c = I_l - I_o \left(e^{\frac{V_c q}{kT_c k}} - 1 \right) \quad (2.2)$$

where:

I_c = cell current (A)

I_l = photo current (A)

G = solar irradiance (W/m^2)

TA = ambient temperature ($^{\circ}\text{C}$)

$I_l = I_l(G)$

$V_c = V_c(G, TA)$

This is the mathematical equation which models the behavior of an ideal photovoltaic cell shown in Figure 2.2 [29]. The production of photocurrent is modeled with a DC current source and the dark current is modeled with a diode referred to as the diffusion diode.

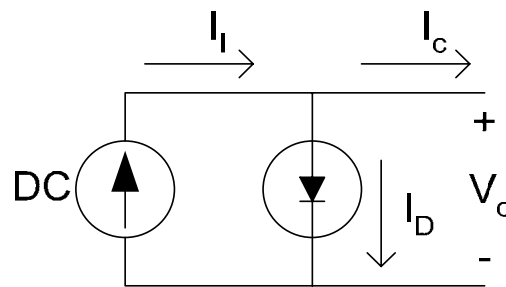


Figure 2.2: Circuit model of an ideal solar cell

Modeling of non-ideal solar cells and the behavior of solar cells under varying environmental conditions will be discussed further in Section 3.2.

2.1.2. The Photovoltaic Module

A photovoltaic module is composed of a series and parallel connection of solar cells, with the additional components of blocking and bypass diodes. While the manufacture and size of solar cells vary, in general a single cell has a relatively low voltage handling capability on the order of 0.6 V [10]. In order to package solar cells as a more practical device most manufacturers produce solar modules; a group of solar cells connected in series and parallel in order to increase the voltage and current handling capability. While a variety of connection schemes exist for a multitude of applications, a common scheme for PHV modules used in grid tied power generation is a connection of 72 cells in series. As an example, the Shell SQ150-PC module which is so composed provides rated voltage and current of 34 V, 4.4 A [10].

In most PHV design and modeling applications the following assumption is made, which is also used in this work:

A1: Connection of solar cells in series will directly multiply the voltage handling capability of the system and connections in parallel will directly multiply current production.

For this assumption to be reasonable it is necessary for all solar cells to behave in a uniform manner (further discussion in Section 3.2.2.), however it is clear that this is not always the case. Solar modules contain blocking and isolation or bypass diodes as shown in Figure 2.3 to reduce the effects of cells which do not act uniformly. Without these devices it is possible for cells or strings which are not operating uniformly to consume power generated by other cells or strings. These devices therefore reduce the power loss

associated with non-uniformity and allow the behavior of the array to more closely resemble the uniform case by reducing the negative impact of non uniform cells.

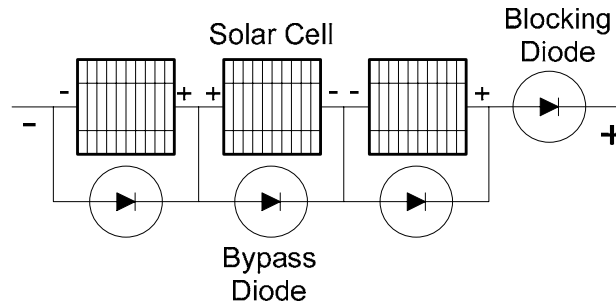


Figure 2.3: String of cells with bypass and blocking diodes

Thus for this work, the following additional assumptions are made:

A2: Each cell behaves in a uniform manner. Under a given environmental condition the electrical characteristics of every cell in a solar array is identical.

A3: For the purposes of modeling a solar array in this work the bypass diodes and isolation/blocking diodes are considered as ideal diodes.

With these assumptions in place, bypass diodes are reverse biased and act as open circuits while isolation or blocking diodes are forward biased and act as short circuits. Therefore it is not necessary to include these diodes in the mathematical model to be described in Chapter 3.

Bypass diode:

Bypass diodes are placed across each cell in a solar module in order to ensure that each series string of cells produces the maximum possible voltage. This protects against the case where a given solar cell does not receive the same illumination as other cells in the string. For example, given a string of cells, if a single cell is covered in dirt and thus absorbs less radiation it is possible for the voltage gain of this cell to reverse its direction

($I_D > I_L$, as shown by the center cell in Figure 2.3) which would significantly reduce the voltage gain of the entire string. Therefore, a bypass diode is connected in parallel to each solar cell which becomes forward biased if the voltage gain of a cell is reversed, and effectively creates a short across this cell. Then, when a cell voltage is reversed the voltage capability of the string is increased by the action of the bypass diode [5].

Isolation/Blocking Diodes:

Isolation or blocking diodes are often placed between each string of modules and the PCU in order to prevent module strings from absorbing power from the system when not illuminated. Under zero illumination and in the presence of forward voltage (provided by a battery, the grid, or other module strings) a string of solar modules will draw current from the circuit [5]. Therefore an isolation or blocking diode is placed between the module string and the voltage source as shown in Figure 2.3. The term blocking diode often refers to a single diode used in PHV systems with battery storage, while isolation diodes refer to multiple diodes placed on the positive terminal of each series string of solar modules. These diodes perform the same function of blocking a reverse current flow however multiple isolation diodes provide additional protection in the case of shading on a single string of modules. These diodes become reversed biased when the string is not illuminated thus preventing current flow to the string. In some cases, the function of a blocking diode is performed by switching in the PCU, however this only prevents the array from absorbing power from the grid, it does not prevent a single module string from absorbing power from the rest of the array.

2.1.3. The Photovoltaic Array

A photovoltaic array is composed of series and parallel connections of solar modules. The number of modules connected in series and parallel is based on the voltage requirements of the system and the desired power output of the array. Grid connected systems require an inverter which in order to successfully interface with the grid requires a specific DC input voltage range generally on the order of 200-600 Volts DC [33]. PHV arrays are designed to produce a voltage close to the top of this range at rated power production. This allows the inverter to operate for the largest possible range of DC voltage input and therefore the largest range of environmental conditions.

Once the voltage requirement is met, power handling capability can be increased by connecting additional module strings in parallel. This is done by first connecting the correct number of modules in series to fulfill the voltage requirement creating a string of modules. Next, additional strings of the same number of modules may be added to increase the current production and thus the power capability of the array. It is important that each string is composed of an identical number of modules of the same brand and power rating. If strings are not matched the voltage production of each string may not be identical. In this case the voltage output of the array will be lower than that of the highest producing string, therefore the highest producing string does not operate at maximum efficiency.

2.1.4. The Power Conditioning Unit

The power conditioning unit (PCU) is a device which interfaces the solar array with the utility grid. In a grid tie system without storage the PCU consists of a maximum power point tracker (MPPT) and a DC to AC inverter, as shown in Figure 2.4. In most

cases the PCU also contains protection devices which disconnect the PHV system from the grid in the case of grid failure. Many PCU's use the existing controllable switches of the DC to AC inverter in order to perform these protective functions. These components are described in detail in the following sections.

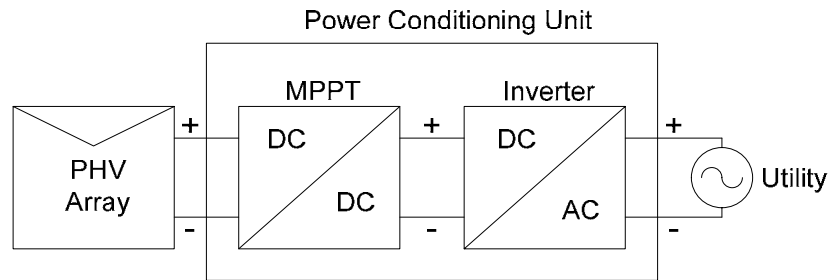


Figure 2.4: Components of the power conditioning unit

2.1.4.1. The Maximum Power Point Tracker

The MPPT is a DC to DC voltage converter which ensures that the PHV array provides the maximum available power to the inverter. Typical I-V characteristics are shown in Figure 2.5 and Figure 2.6 where environmental conditions are varied. As can be seen in the figures, a solar array is able to provide constant current for a range of voltages below a given threshold, where the maximum power point occurs just beyond this threshold. The MPPT device assures that the input to the inverter remains constant at this optimal operating point. A variety of DC to DC converters such as buck, boost, buck-boost, or Cúk can be used for this function [7].

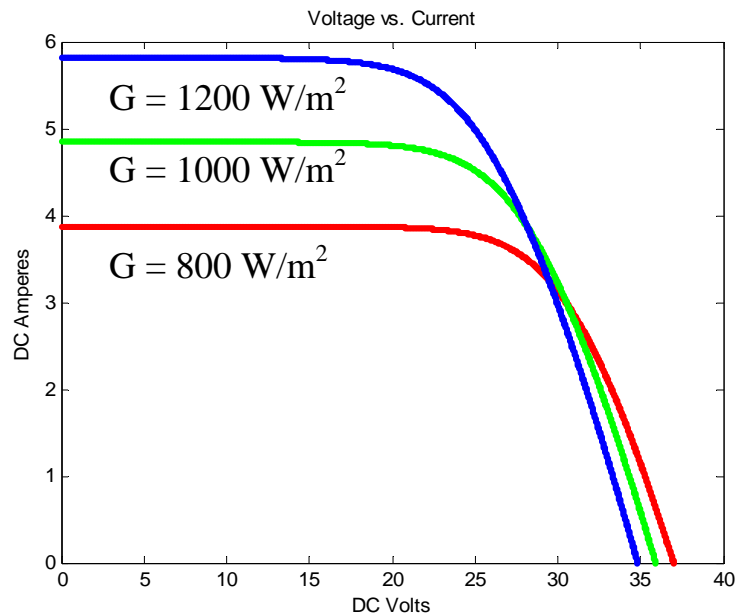


Figure 2.5: I-V Characteristic of a solar module under varied solar irradiance

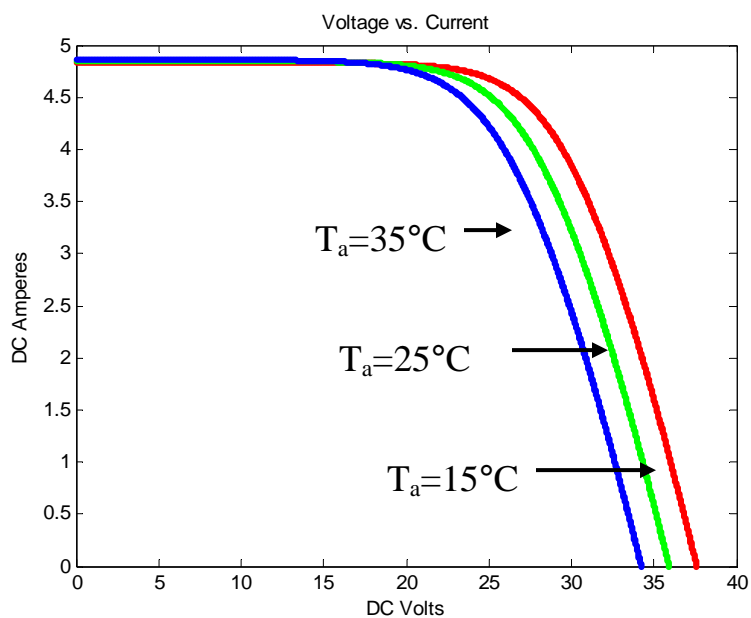


Figure 2.6: I-V Characteristic of a solar module under varied ambient temperature

2.1.4.2. The DC to AC Inverter

The DC to AC voltage converter ties the DC output of the MPPT with the AC bus of the utility grid. Most grid tie PCU's use self-commutated voltage source inverters

which are built with switching devices such as IGBT's or MOSFET's. These types of switches have the advantage of allowing control of both the on and off switching events. This characteristic is optimal for normal DC to AC inverter operations and in addition allows for the existing switches of the inverter to be used for protection functions. Thus the self-commutated inverter can provide control of the power factor and suppression of harmonic current, as well as protection against grid disturbance. The self-commutated inverter is capable of executing two separate control schemes, current control and voltage control. The control scheme is selected based on the size and function of the PHV generator.

The current control scheme is the most widely used scheme for grid tied PHV generators. This is because of its ability to provide a very high power factor with simple control circuitry [14]. This scheme senses the voltage waveform of the grid for a reference value and matches the phase angle of the current output to the reference within a certain tolerance. A high power factor results because the current phase is controlled to match the phase of the grid. The current control scheme is ideal for residential and small commercial PHV generators where control of the bus voltage magnitude is not necessary; however, a high power factor and reduced cost of the inverter are priorities.

The voltage control scheme is used for most off grid applications and some grid tied applications where it is desired to control the voltage magnitude of the AC bus. This scheme taps the grid for a reference and matches the voltage output to the reference within a certain tolerance. A PWM control scheme is utilized resulting in a waveform with less lower-order harmonic components [14]. Control of the output voltage is necessary for off grid applications where the PHV generator is the only source of power

in the circuit. In this case, it is necessary for a certain voltage magnitude to be maintained by the generator for proper operation of the loads and storage devices which rely on the PHV generator for power. Large commercial or industrial grid tied PHV generators may also use this scheme in order to control the voltage magnitude of the output bus. The power output of a PHV system varies over a wide range in a single day, and the power injected to the grid will affect the voltage at the output bus. Therefore, large PHV generators could create undesirable swings in the voltage level at the output bus including significant over voltage levels. In order to prevent a large PHV generator from causing such disturbance problems in the grid a voltage control scheme can be utilized in the inverter. With this scheme the voltage magnitude of the output bus is maintained regardless of the power output which prevents the PHV generator from causing voltage swings in the grid.

The type of control scheme selected for a given PHV generator will determine the generator modeling scheme to be used when integrating with an unbalanced power flow analysis. Utilizing the current control scheme will cause a PHV generator to be modeled as a constant PQ power source while use of the voltage control scheme will result in a constant P|V| power source model. This is discussed further in Chapter 4.

2.2. Unbalanced Distribution Power Flow

The goal of this work is to study the affect PHV generators will have on the utility distribution grid. PHV generators are often single phase devices which produce power at low voltage levels. These characteristics match well with distribution systems which allow for single and two phase feeders and distribute power at mid to low voltage levels, therefore a majority of PHV generation systems are connected to the distribution system.

Thus unbalanced distribution power flow analysis is most appropriate for performing the desired studies.

Distribution systems are unbalanced networks which can contain single phase or two phase feeders and are often characterized by a radial or tree structure. Figure 2.7 shows the basic building block of a distribution power system which interconnects several components. The unique characteristics of distribution systems require detailed, unbalanced component models for elements such as lines, switches, and transformers to be used in distribution power flow methods [35].

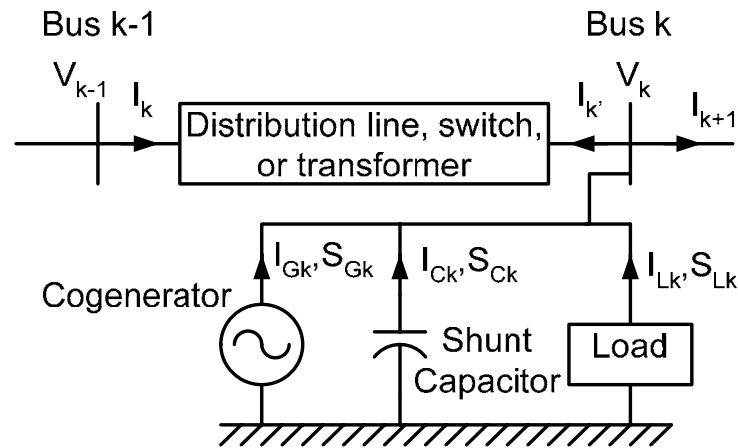


Figure 2.7: The basic building block of a distribution system [36]

Each component can have up to three phases therefore the variables in Figure 2.7 are vectors with up to three elements, and the following notation is defined:

V_{k-1} = steady state voltage at bus k-1

V_k = steady state voltage at bus k

I_k = steady state current flow from bus k-1 to bus k

I_k = steady state current flow from bus k to bus k-1

$I_{(G,C,L)k}$ = steady state current injection at bus k

$S_{(G,C,L)k}$ = steady state power injection at bus k

Devices connected to a bus such as multi-phase loads, co-generators and capacitors can be modeled as current or power injections to the network [36] as shown in Figure 2.7. Two common methods for solving power flow include backward/forward sweep techniques for radial structure systems and Newton Raphson for general structured systems. Each implementation utilizes the multi-phase component modeling in [35] and each method solves for the steady state voltages at the existing phases concurrently.

A brief discussion of select co-generator models for both the backward/forward sweep and Newton Raphson methods is provided. The two main types of generator models are constant PQ sources and constant P|V| sources, which will now be discussed in detail respectively.

2.2.1. Constant PQ sources

Co-generators are commonly modeled as constant power devices. In general, synchronous generators are controlled to maintain constant power output and constant power factor. Some utilities require that a power factor controller must be able to maintain the power factor within plus or minus one percent [6]. Induction co-generators are not able to control their power factor as the reactive power will vary with the terminal voltage. For induction generators the use of a constant PQ model is considered a simplification based on the assumption of a constant bus voltage [6]. Therefore in this model, power output of the device is determined completely by its own characteristics and operations and is independent of the behavior of the utility grid to which it is connected.

Backward/Forward Sweep:

While the power output remains constant the current output of the device is dependent on the bus voltage magnitude to which it is connected [36]. The current injection due to a co-generator connected to bus k is calculated in (2.3):

$$I_{Gk} = \left(\frac{S_{Gk}}{V_k} \right)^* \quad (2.3)$$

where:

S_{Gk} = power supplied by co-generator at bus k

I_{Gk} = current injection due to co-generator at bus k

Newton Raphson:

In the traditional Newton Raphson method load busses are modeled as constant power PQ busses. It is assumed that the power injection at a load bus is known, which is key because the mismatch equation for Newton Raphson is defined as the difference between the known values for power injection and the values for power injection calculated from the variables at each iteration. Therefore when a PHV generator is connected to a load bus the power generated is added to the known power consumption before the power flow is performed [11].

2.2.2. Constant P|V| Sources

Some generators do incorporate control schemes which allow the generator to regulate the terminal voltage to a specified value. In this case, the reactive power output of the generator is determined by the behavior of the grid to which it is connected.

Backward/Forward Sweep:

For this scheme to be modeled it is necessary to calculate the reactive power output required to maintain the specified voltage at the given real power output. One method [26] creates a fictitious node and branch which feeds reactive power to the specified P|V| node thus maintaining the desired voltage value. Using this technique the P|V| node can actually be treated as a PQ node in calculations where the Q injection is calculated from [26]:

$$Q_k = |V_k^t| \left(\frac{V_{fic,k}^t - |V_k^t|}{X_{fic,k}} \right) \quad (2.4)$$

where:

Q_k = specified value of reactive power injection at bus k

V_k^t = calculated voltage value in bus k at iteration t

$V_{fic,k}^t$ = calculated voltage of fictitious node of bus k at iteration t

$X_{fic,k}$ = fictitious branch impedance of bus k

In the case of generators which are connected to the grid through an inverter the available injection current is limited. If the Q value determined in (2.4) violates the current constraint then the inverter will not be able to maintain the specified voltage and control is switched to current control which is modeled by the constant PQ source model. The Q limit is determined by [26]:

$$Q_{k,\text{lim}} = \pm \sqrt{S_{Gk}^2 - P_k^2} \quad (2.5)$$

where:

S_{Gk} = power produced by the generator at bus k

P_k = specified real power output of the generator at bus k

Newton Raphson:

In the traditional Newton Raphson method, busses connected to generators are modeled as constant $P|V|$ busses. The known value for the real power injection is included in the mismatch equation and the unknown reactive power value is not. The bus voltage magnitude is specified and thus is not included as a variable. A limit is placed on the reactive power that may be produced by the generator and after each iteration the reactive power output is calculated and compared to the limit value. If the constraint is violated the power flow is considered invalid because no solution exists which satisfies the both the reactive power limit and the voltage magnitude requirement [11].

Given the concepts reviewed in this chapter, development of a PHV array model is presented in the following chapter. Integration of the PHV array model with an unbalanced distribution power flow analysis is described in subsequent chapters.

3. Photovoltaic Array Model

This chapter develops a model which calculates the DC power output P_G^{DC} , of a photovoltaic array as a function of the array ratings and a set of environmental conditions:

$$P_G^{DC} = P_G^{DC}(\text{array ratings, environmental conditions}) \quad (3.1)$$

The model is intended for use by system planners and operators who will have a limited amount of data available to them regarding the photovoltaic systems themselves, and the environmental conditions which determine their output. Inputs corresponding to the solar modules are limited to the information available on a typical specification sheet, such as those shown in Appendix D. Inputs corresponding to the size and connection scheme of an array are limited to a power rating. Inputs corresponding to the environmental conditions are limited to solar irradiance which determines current production and ambient temperature which most heavily impacts the voltage handling capability. A list of the inputs to the model is shown below:

(1) Array power rating:

$$P_{ra} = \text{rated DC power output of the array (W)}$$

(2) Solar module specifications:

$$V_{ocM} = \text{module open circuit voltage (V)}$$

$$I_{scM} = \text{module short circuit current (A)}$$

$$(I_{mM}, V_{mM}) = \text{module maximum power point (A, V)}$$

$$P_{rM} = \text{module rated power output (W)}$$

$$NOCT = \text{nominal operating cell temperature (}^\circ\text{C)}$$

$$\left(\frac{\partial I_{scM}}{\partial T_c} \right), \left(\frac{\partial V_{ocM}}{\partial T_c} \right) = \text{temperature coefficients}$$

$$N_{cs} = \text{number of cells in series in the module}$$

(3) Environmental conditions:

G = solar irradiance (W/m^2)

T_A = ambient temperature ($^{\circ}\text{C}$)

Figure 3.1 shows an I-V curve of a solar module with the three points commonly provided on specification sheets. In this chapter, the characteristic equation of the non-ideal photovoltaic cell will be presented first, followed by the method used to scale the equation to represent an entire array. A step by step summary of the modeling procedure is then provided, which is followed by subsections containing detailed explanations. A flow chart of the modeling procedure is then shown which specifies the inputs and output of each step is shown. Finally the implementation of the PHV array model is described and the results of an example calculation are presented.

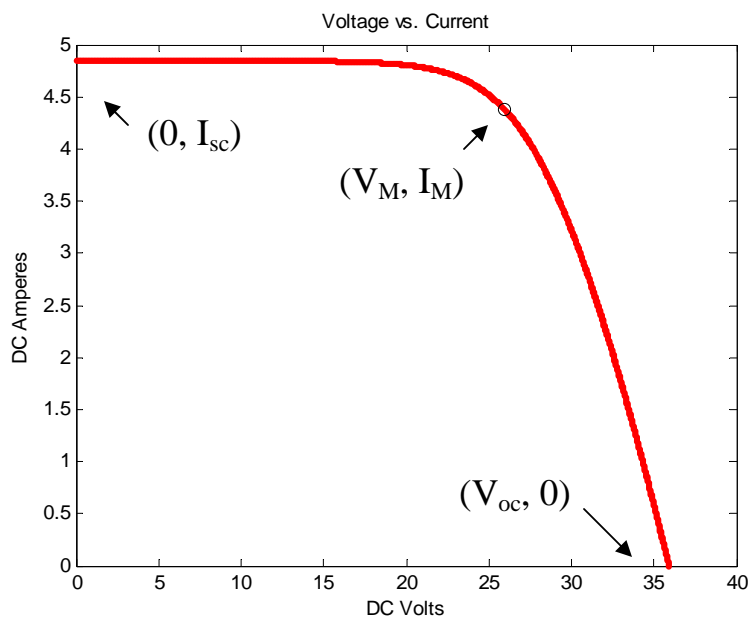


Figure 3.1: I-V curve showing the three points given on a typical specification sheet.

3.1. Characteristic Equation of the Non-Ideal Photovoltaic Cell

The circuit model of a photovoltaic cell often used for research purposes is shown in Figure 3.2. This model was selected due to its use of specification sheet inputs, and its appearance in several texts regarding photovoltaic devices [5, 20, 29].

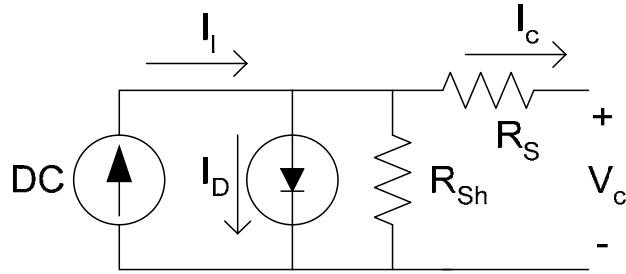


Figure 3.2: Electrical model of a solar cell with shunt resistance

In addition to the components of the ideal model, the model shown incorporates a series and shunt resistance to capture the behavior of a physical solar cell more accurately. Several elements of the solar cell contain resistive properties such as the semiconductor material itself, the metal grid which collects current from the semiconductor material, the collector bus and the internal wiring. It is assumed that these series losses can be modeled using a lumped resistor R_s . Several shunt resistive losses occur such as localized shorts at the emitter layer of the semiconductor material and perimeter shunts at the cell borders. The combined effect of these shunts is modeled by a lumped parallel resistor R_{sh} . Equation 3.1 describes the I-V characteristic of this cell model:

$$I_c = I_l - I_o \left(e^{\frac{(V_c + I_c R_s)q}{nkT_c k}} - 1 \right) - \frac{V_c + I_c R_s}{R_{sh}} \quad (3.1)$$

where:

I_c = cell current (A)
 I_{sc} = cell short circuit current (A)
 I_l = cell photo-current (A)
 I_o = saturation current of the diode (A)
 V_c = cell voltage (V)
 R_s = series resistance
 R_{sh} = shunt resistance
 $q = 1.6 * 10^{-19}$ (coul)
 $k = 1.38 * 10^{-23}$ (j / K)
 T_{cK} = Cell Temperature (K)
 n = nonideality constant of the diode
 Note: $I_l = I_{sc}$

It is shown in [5] that only very small values of R_{sh} will significantly affect the power output of the model. Solar cells are designed to reduce shunt losses and therefore most commercially available solar modules have relatively large shunt resistances. Thus this work will make the following assumption:

A4: the shunt resistance can be neglected:

$$R_{sh} = \infty \quad (3.2)$$

This results in the equivalent circuit model shown in Figure 3.2.

Also, it is not possible to consistently calculate a value for R_{sh} given the available parameters listed in Section 3.3. R_{sh} is determined by the slope of the I-V curve at the short circuit point [29]:

$$\frac{dI}{dV}_{v=0} = -\frac{1}{R_{sh}} \quad (3.3)$$

For this calculation to be made accurately, empirically determined I-V characteristic curves must be available. Therefore the model will be modified according to (3.2) which may result in a bias that overestimates the power production of the solar array.

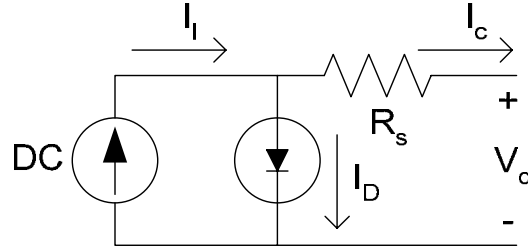


Figure 3.3: Model of a solar cell without shunt resistance

$$I_c = I_l - I_o \left(e^{\frac{(V_c + I_c R_s)q}{nkT_c k}} - 1 \right) \quad (3.4)$$

Figure 3.3 depicts the model of a solar cell neglecting the effects of shunt resistance. (3.4) describes the electrical behavior of this circuit. This is the circuit model that will be used to simulate the behavior of a solar cell in this thesis. All of the parameters of (3.4) can be determined from the input parameters listed. This equation is the basic building block of the array model just as the solar cell is the building block of an actual array. The equation must now be modified in order to model the behavior of a photovoltaic array.

3.2. Conversion of Cell Characteristic Equation to Array Characteristic Equation

In order to model a solar array, a circuit composed of series and parallel connections of solar cells as shown in Figure 3.4 is utilized. For the purpose of modeling an array an assumption is made that the current and voltage characteristics of each cell in the array is uniform (A3). This is important for two reasons: First, it ensures the bypass

diodes will be reverse biased and are treated as open circuits and the blocking diode is forward biased and is treated as a short. Second, it ensures that the exponential expression (3.4) may be scaled in a linear manner based on the series and parallel connection of cells because the parameters in the exponent (V_c , I_c , T_{ck}) will be identical for each cell.

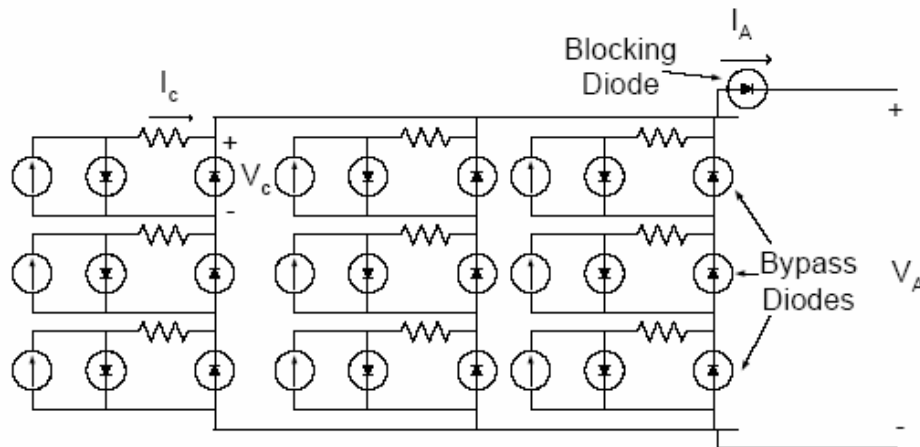


Figure 3.4: Circuit diagram of a 3x3 solar array

Where with ideal blocking and bypass diodes:

$$I_A = \text{array current (A)}$$

$$V_A = \text{array voltage (A)}$$

The following simplifying assumption is made:

A5: A solar module is composed only of series connections of solar cells.

Many solar modules used for grid tie systems are composed of 72 cells connected in series [10]. This assumption greatly simplifies the modeling procedure and the characteristic equation that is used as the final model of the array. With this assumption in place, an array can be simply described as an $N_s \times N_p$ grid of cells as shown in Figure

3.4 where N_s describes the number of cells in a string and N_p describes the total number of strings in the array. While it is true that modules exist which contain parallel cell connections, these are generally used for low voltage applications such as stand alone DC systems with battery storage and are not utilized for grid connected photovoltaic generators.

Given that in a series connection voltages sum and in a parallel connection currents sum the following relations apply:

$$\begin{aligned}
 I_A &= N_p I_c \\
 I_{scA} &= N_p I_{sc} \\
 V_A &= N_s V_c \\
 V_{ocA} &= N_s V_{oc}
 \end{aligned} \tag{3.5}$$

where:

$$\begin{aligned}
 N_s &= \text{number of cells connected in series} \\
 N_p &= \text{number of cells connected in parallel} \\
 I_{scA} &= \text{short circuit current of the array (A)} \\
 V_{ocA} &= \text{open circuit voltage of the array (V)}
 \end{aligned}$$

Remembering that $I_l = I_{sc}$ and substituting these into equation (3.4) results in:

$$I_A = I_{scA} - N_p I_0 \left(e^{\frac{(V_A + I_A R_{scA})q}{nN_s k T_{cK}}} - 1 \right) \tag{3.6}$$

The scheme presented above is a commonly accepted method for scaling the cell characteristic equation in order to form the array characteristic equation [5]. Inputs to the model developed here include parameters related to solar modules instead of single cells

and thus this scaling method must be modified to account for module inputs. This is described in section 3.3.2.

3.3. Step by Step Modeling Procedure

In order to develop the model parameters basic steps are outlined below. Detailed discussions of each step are contained the subsections.

Step 1) Determine the connection scheme of the array (Section 3.3.1).

Step 2) Convert the cell characteristic equation to an array characteristic equation (Section 3.3.2.).

Step 3) Solve for parameters of the characteristic array equation (Section 3.3.3.).

Step 4) Calculate the I-V curve of the characteristic equation and determine P_G^{DC} (Section 3.3.4.).

3.3.1. Determine the Connection Scheme of the Array:

The array connection scheme refers to the number of solar modules connected in series to form a string and the number of parallel strings used to form the array. The array characteristic equation requires the module connection scheme in order to specify (N_s, N_p) , however this information is not available therefore the model determines an appropriate connection scheme from the desired power rating and equipment specifications. In many cases the only information a system planner/operator will have concerning the connection scheme will be the rated power output P_{rA} of the array. However since the mathematical model is built by scaling the equation of a single solar cell to describe an array, a specific connection scheme is needed. Therefore, the following procedure of (3.7) has been developed to determine the probable connection scheme:

$$\begin{aligned}
N_{sM} &= \text{ciel}(V_{DC} / V_{mM}); \\
P_{Col} &= N_{sM} \cdot P_{rM}; \\
N_{pM} &= \text{ciel}(P_{rA} / P_{Col}); \\
\text{Actual}P_{rA} &= N_{sM} \cdot N_{pM} \cdot P_{rM};
\end{aligned} \tag{3.7}$$

where:

$$\begin{aligned}
\text{ciel}() &= \text{function that rounds to the next highest integer} \\
V_{DC} &= \text{The desired nominal DC voltage (usually 500V)} \\
N_{sM} &= \text{Number of modules in series required to achieve } V_{DC} \\
P_{Col} &= \text{Power rating of a single string of } N_{sM} \text{ modules} \\
N_{pM} &= \text{number of series strings connected in parallel required to achieve } P_{rA}
\end{aligned}$$

First the minimum number of series modules, N_{sM} , required to achieve the desired voltage output at rated operation is determined. Second, the power rating of this string of modules, P_{Col} , is calculated, and third, the minimum number of strings required to achieve the desired power, N_{pM} , is determined. Fourth, the actual power rating of the system that will be integrated with the power flow is calculated.

This scheme builds a PHV array in a discrete manner, as the power rating of the overall array can only be increased in steps corresponding to the size of the power rating of a single string of modules. Thus, for an arbitrary desired power rating, this scheme designs an array with a rating greater than or equal to the rating input by the user. The method is considered conservative for system studies since the effects of PHV generation, such as phase imbalance, and overall demand curve changes increase as the PHV system rating increases. It is noted that the power rating used in the power flow solution is bounded because the over estimate does not exceed the rated power of a single string of modules. The size of a single string of modules is limited because it is based on the input DC voltage range of the power conditioning device. The effect of

overestimation is significantly reduced by the fact that in utility-based distribution power flows each bus typically represents an aggregate bus such as a pole top transformer which services a number of loads. Therefore the PHV system on a given bus represents the aggregate of all the PHV systems serviced by that bus, and for this aggregate system the overshoot is limited to a single string of module.

3.3.2. Convert the Cell Characteristic Equation to an Array Characteristic Equation

Once the connection scheme is determined the characteristic equation must be scaled up to describe the behavior of the entire array. This is done according to (3.5) and (3.6) however it is important to note that values for I_{sc} , V_{oc} , and P_r are given at the module level. Therefore, the procedure is modified to scale appropriately from the module level to the array level:

$$\begin{aligned} I_{scA} &= I_{scM} \cdot N_{sM} \\ V_{ocA} &= V_{ocM} \cdot N_{sP} \\ P_{rA} &= N_{sM} \cdot N_{sP} \cdot P_{rM} \end{aligned} \quad (3.8)$$

The number of cells in series is the product of the number of series cells in the module, N_{cs} , and the number of modules in the string, N_{sM} . The number of parallel connections of cells is simply the number of parallel strings of modules:

$$\begin{aligned} N_s &= N_{cs} \cdot N_{sM} \\ N_p &= N_{sP} \end{aligned} \quad (3.9)$$

Once these calculations have been performed the appropriate substitutions can be made in (3.10). This is the form of the I-V characteristic equation that will be used to model the photovoltaic array:

$$I_A = I_{scA} - N_p I_0 \left(e^{\frac{(V_A + I_A R_{sA})q}{nN_s k T_c k}} - 1 \right) \quad (3.10)$$

3.3.3. Solve for parameters of the characteristic array equation

- Calculate the series resistance of the array R_{sA}
- Calculate the array open circuit voltage and short circuit current at the given environmental conditions
- Calculate the saturation current of the diffusion diode I_0

Calculate the series resistance of the array R_{sA} :

The series resistance of the array is modeled as a single lumped resistor as is appropriate given assumption A2. While specifications sheets for solar modules do not provide a value for the series resistance a value for the series resistance can be calculated from the parameters that are provided, the key parameter being the maximum power production at standard test conditions. Parameters needed from previous calculations to calculate series resistance are $(V_{ocA}, I_{scA}, P_{rA})$. Note that these parameters refer to the entire array. Thus the series resistance of the entire array will be calculated directly.

In addition, the following calculations will make use of the parameter fill factor defined as follows:

$$FF_A = \frac{V_{rA} I_{rA}}{V_{ocA} I_{scA}} \quad (3.11)$$

The fill factor of a given array describes the relationship between the rated power output and the product of the short circuit voltage and open circuit voltage. While the fill factor is not strictly a measure of efficiency it is indicative of the efficiency of the array. This measure is useful because it is possible to approximate FF_{0A} defined as the fill factor of an array where $R_{sA} = 0$, using the empirical relationship in (3.12):

$$FF_{0A} = \frac{v_{oc} - \ln(v_{oc} + 0.72)}{1 + v_{oc}} \quad (3.12)$$

$$v_{oc} = \frac{V_{ocA} q}{N_s n k T_{cK}}$$

where:

FF_0 : Fill Factor of the array without a series resistance

The key to the following derivation is that (V_{ocA}, I_{scA}) remain the same in the two cases of an array with and without series resistance. This allows us to define a relationship between (3.11) and the empirically determined [5] (3.12) which involves the parameter of series resistance. The derivation for the value of R_{sA} will now be described:

$$P_{rA} = V_{rA} I_{rA}$$

$$P_{rA} = P_{rAwoR} - I_{rA}^2 R_{sA}$$

$$P_{rA} = P_{rAwoR} \left(1 - \frac{I_{rA}}{V_{rA}} R_{sA} \right) \quad (3.13)$$

$$\frac{I_{rA}}{V_{rA}} \approx \frac{I_{scA}}{V_{ocA}}$$

where:

$$P_{rAwoR} = \text{Denotes power the array would output if } R_{sA} = 0$$

$$(V_{rA}, I_{rA}) = \text{Voltage and current of the array at rated power}$$

The approximation shown in (3.13) is an assumption based on the shape of the I-V characteristic of the solar cell.

$$P_{rA} = P_{rAwoR} \left(1 - \frac{I_{scA}}{V_{ocA}} R_{sA} \right)$$

$$FF = \frac{P_{rA}}{V_{ocA} I_{scA}} = \frac{P_{rAwoR} \left(1 - \frac{I_{scA}}{V_{ocA}} R_{sA} \right)}{V_{ocA} I_{scA}} = FF_0 \left(1 - \frac{I_{scA}}{V_{ocA}} R_{sA} \right) \quad (3.14)$$

Now solve for R_{sA} :

$$R_{sA} = \frac{V_{ocA}}{I_{scA}} - \frac{P_{rA}}{FF_{0A} I_{scA}^2} \quad (3.15)$$

Alternative methods for the calculation of series resistance do exist [29]. This method requires the use of many empirically determined I-V characteristics of the solar module or array and therefore is impractical for use in this algorithm because the detailed information required is often unavailable.

Calculate the array open circuit voltage and short circuit current at the given environmental conditions:

This section describes how the short circuit current and open circuit voltage of the array are transformed from rated values (I_{scAr} , V_{ocAr}) to the appropriate values given the environmental state (I_{scAE} , V_{ocAE}). I_{scAE} is substituted directly into (3.10) and both (I_{scAE} ,

V_{ocAE}) are used to calculate the saturation current of the diode I_0 later in this section. While the short circuit current and open circuit voltage do not describe operating points of a solar generator during normal operation, the operating points are determined from these parameters. Therefore, for purpose of discussion it is appropriate to assume that the impact environmental conditions have on the short circuit current and open circuit voltage will be similar to the effect on the operating current and voltage respectively of the array.

The rated values (I_{scM} , V_{ocM}), are determined empirically at standard test conditions (3.16) and published in the specification sheet of the module:

$$\begin{aligned} G &= 1000 \text{ W/m}^2 \\ T_A &= 25^\circ\text{C} \\ \text{Atmospheric Spectrum} &= \text{AM 1.5} \end{aligned} \tag{3.16}$$

The current produced by a solar cell is directly dependant on the solar irradiance incident upon its surface. The current produced by the array is proportional to the energy input in the form of solar irradiance. The array output voltage is heavily impacted by the temperature of the solar cell because the voltage handling capability of the semiconductor material is dependant on the temperature of the material.

The nominal operating cell temperature or NOCT is a value determined empirically under a separate set of standard test conditions of 800 W/m^2 , 20°C , AM 1.5. It is used to calculate the cell temperature as a function of ambient temperature:

$$T_c = T_a + \frac{NOCT - 20}{800} \cdot G(\text{W/m}^2) \tag{3.17}$$

As shown in (3.18) the energy output in the form of current is directly proportional the energy input in the form of solar irradiation. There is a small temperature coefficient, $\left(\frac{\partial I_{scA}}{\partial T_c}\right)$, on the order of a few milliamps per degree Celsius to account for temperature differences recognized empirically.

$$I_{scAE} = \frac{I_{scAr}}{1000} G + \left(\frac{\partial I_{scA}}{\partial T_c}\right) (T_c - T_{c0}) \quad (3.18)$$

where:

T_c = Cell temperature (°C)

T_{c0} = Cell temp at standard test conditions (usually 25°C)

T_A = Ambient temperature (°C)

$NOCT$ = Nominal Operating Cell Temperature

A_r = Denotes rated (max power point at standard test conditions) value of the array

A_E = Denotes value for the array at given environmental conditions

The open circuit voltage of the array under given environmental conditions is calculated in (3.19):

$$V_{ocAE} \approx V_{ocAr} + \left(\frac{\partial V_{ocA}}{\partial T_c}\right) (T_c - T_{c0}) + \frac{kT_{cK}}{q} \ln\left(\frac{I_{scAE}}{I_{scAr}}\right) \quad (3.19)$$

As the temperature of the cell rises, the voltage capability of the semiconductor material in the cell is diminished and thus the voltage across the cell decreases. This can be determined through manipulation of the PHV characteristic equation. A temperature

coefficient is inserted to account for empirically determined effects. A derivation of this equation is included in Appendix B.

The values for open circuit voltage and short circuit current at the given environmental conditions are thus determined [5]. These values will now be used to solve for the saturation current of the diffusion diode.

Determination of the saturation current of the diffusion diode I_0 :

With substitutions made for operation under given environmental conditions (3.10) can be written as:

$$I_A = I_{scAE} - N_p I_0 \left(e^{\frac{(V_A + I_A R_{sA})q}{nN_s k T_{cK}}} - 1 \right) \quad (3.20)$$

The parameter I_0 is determined by setting the equation to open circuit conditions, and solving for I_0 :

$$\begin{aligned} I_A &= 0 \\ V_A &= V_{ocAE} \\ I_0 &= \frac{I_{scAE}}{N_p \left(e^{\frac{V_{ocAE}q}{nN_s k T_{cK}}} - 1 \right)} \end{aligned} \quad (3.21)$$

3.3.4. Calculate the I-V Curve of the Characteristic Equation and Determine P_G^{DC}

The characteristic equation that is used to model the PHV array is repeated in (3.22):

$$I_A = I_{scAE} - N_p I_0 \left(e^{\frac{(V_A + I_A R_{SA})q}{nN_s k T_{cK}}} - 1 \right) \quad (3.22)$$

The variable I_A occurs twice in (3.22), and therefore there is no unique solution to this equation. In order to find the correct solution a known initial condition is required. This model uses the open circuit point ($0, V_{ocAE}$) for this purpose. It can be determined by setting the value of I_A to zero in (3.22):

$$V_{ocAE} = \left(\frac{nN_s k T_{cK}}{q} \right) \ln \left(\frac{I_{scAE}}{I_0 N_p} + 1 \right) \quad (3.23)$$

With ($0, V_{ocA}$) as the initial solution the iterative technique in (3.24) is used to calculate the I-V characteristic of the photovoltaic array:

$$\begin{aligned} &V_A = V_{ocAE}; \\ &I_{A1} = 0; \\ &\text{while } V_A > 0 \\ &\quad V_A = V_A - \text{small_step}; \\ &\quad I_A = I_{scA} - N_p I_0 \left(e^{\frac{(V_A + I_{A1} R_{SA})q}{nN_s k T_{cK}}} - 1 \right); \\ &\quad \text{while } \text{abs}(I_{A1} - I_A) > \text{epsilon} \\ &\quad \quad I_{A1} = I_{A1} + (I_A - I_{A1})/10; \\ &\quad \quad I_A = I_{scA} - N_p I_0 \left(e^{\frac{(V_A + I_{A1} R_{SA})q}{nN_s k T_{cK}}} - 1 \right); \\ &\quad \text{end} \\ &\quad I_{A1} = I_A; \\ &\text{end} \end{aligned} \quad (3.24)$$

As can be seen from (3.24) the initial solution for I_A is input to the equation as I_{AI} . The value of V_A is reduced by small step and iterations are performed until the values of I_A and I_{AI} are within a given tolerance epsilon. Once a solution is determined the procedure is repeated until the short circuit point is reached. I-V curves are thus formed for a solar array given any environmental conditions.

A power vector is calculated from the I-V curve by multiplying the stored vectors of I and V. The DC power output of the array is then defined as the maximum element of the power vector:

$$\begin{aligned} \hat{P} &= \hat{I}\hat{V} \\ P_G^{DC} &= P_{\max AE} = \max(\hat{P}); \end{aligned} \quad (3.25)$$

It is assumed that the PHV array operates at the maximum power point. In the physical system the output of the array may not be the maximum power point however the PHV output is fed to the MPPT which assures the maximum power point is fed into the DC to AC inverter. Therefore the described model accounts for the behavior of both the PHV array and the MPPT. The power loss in the MPPT is taken into account using the efficiency parameter of the PCU as described in Chapter 4.

3.4. Flow Diagram of Procedure for Calculating Power Output of PHV Array

The flow diagram shown in Figure 3.5 describes the PHV array model by defining the equations that are implemented in the model and their input output relationships.

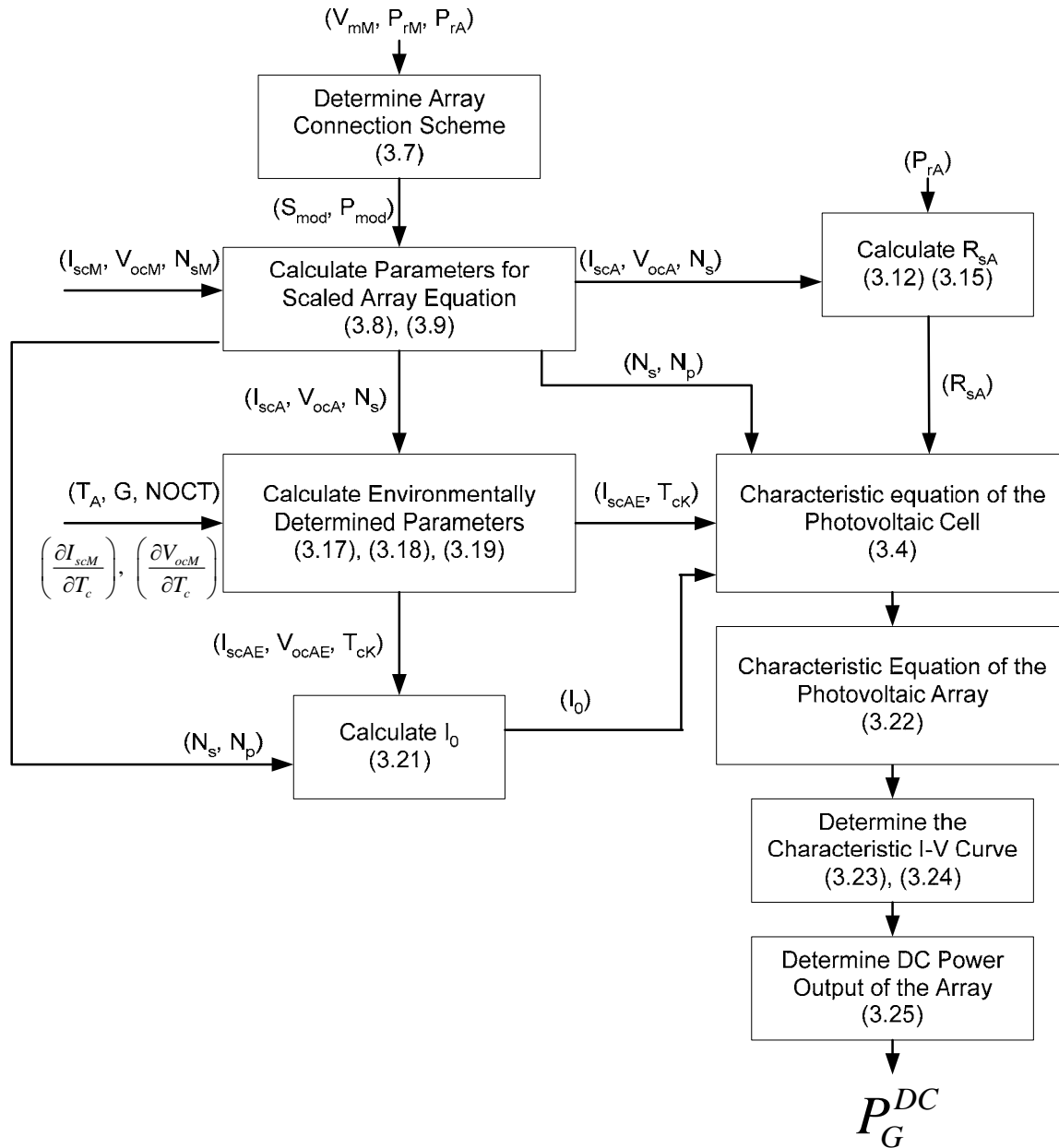


Figure 3.5: Flow diagram of PHV array model

3.5. Implementation and Example

This model has been implemented in MATLAB in order to interface with the software developed in [35]. The output of the model for an example PHV array is presented here in order to describe a typical residential system under a given set of environmental conditions. Figures 3.6 and 3.7 show a typical PHV array I-V curve and PV curve respectively. System specifications are described below:

- 4500 Watts rated PHV Array
- Shell SQ 150 W Modules [4]
- 2 series strings of 15 modules each
- Ambient temperature: 22°C
- Solar irradiance: 850 W/m²
- 26.9 m² total solar module area
- Xantrex GT-3.8 PCU, $\eta = 95.7\%$

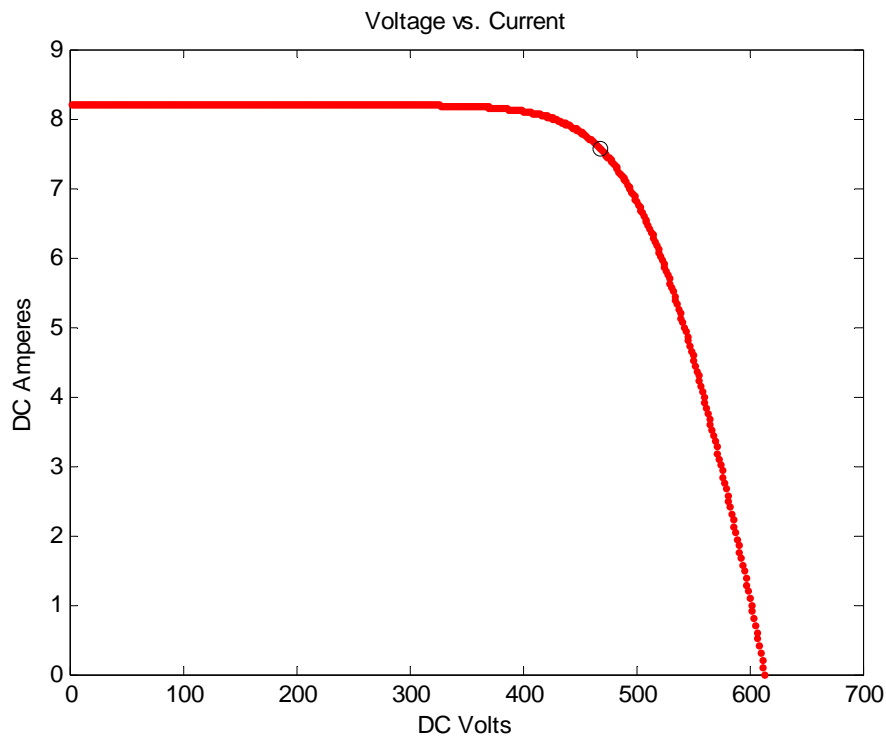


Figure 3.6: I-V Characteristic of example PHV Array (circle denotes max power point)

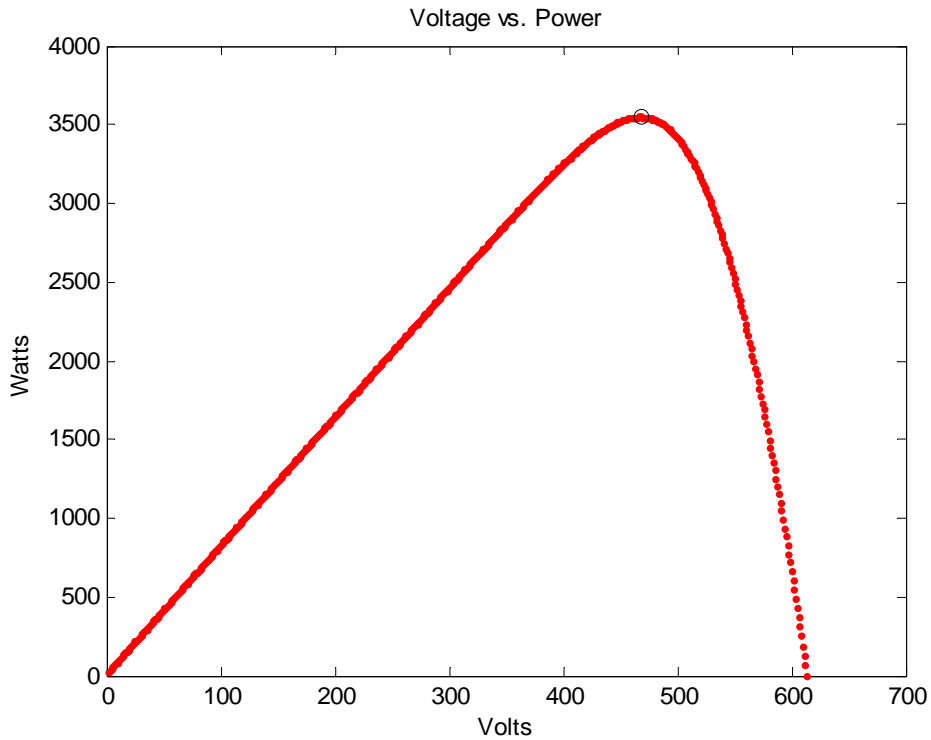


Figure 3.7: P-V Characteristic of example PHV Array (circle denotes max power point)

Notice from Figure 3.5 that the operating voltage of the array is ~ 470 V, which is within the ideal operating range of the inverter (195-550 V) [7]. The power output of this array under the given conditions is 3544.3 Watts DC. Power output of a PHV array varies based on the environmental conditions, and is most often less than the rated output which describes laboratory testing conditions. Chapter 5 contains extensive simulations using various environmental conditions.

4. Model of the Power Conditioning Unit and Integration with Power Flow

This chapter will present the conversion of the PHV array output power P_G^{DC} to an AC power injection S_G^{AC} to the grid dependant on the source model selected:

$$\begin{aligned} \text{PQ: } & S_G^{AC} (P_G^{DC}, \eta, \text{ assumed pf}) \\ \text{P|V|: } & P_G^{AC}, Q_{G,\text{lim}}^{AC} (P_G^{DC}, \eta) \end{aligned} \quad (4.1)$$

where:

S_G^{AC} = complex power injection by PHV generator

P_G^{AC} = real power injection by PHV generator

$Q_{G,\text{lim}}^{AC}$ = limit of the reactive power injection by the PHV generator

η = efficiency of the PCU

pf = power factor

As discussed in Chapter 2 there are two control schemes available for the inverter of the PCU which correlate to two distinct generator models, the PQ source model and the P|V| source model. If the constant PQ source model is selected the complex power injection S_G^{AC} is completely determined by the characteristics of the PHV model. If the constant P|V| model is selected the real power injection and voltage magnitude of the output bus are determined while the reactive power injection is determined by power flow computations. A reactive power limit is also calculated in order to assure the current production capabilities of the PHV generator are not exceeded. PHV generators are often connected at the load site as most PHV generators are owned by individual consumers. Section 4.2 describes how the calculated power injections are integrated with the model of the existing distribution system for power flow analysis.

4.1. Power Conditioning Unit Modeling

Most PHV generators utilize self commutated voltage source inverters and the inverter control scheme used in the PCU of the PHV generator determines the generator model to be implemented. Generators which utilize current controlled inverters are modeled as constant PQ sources and generators which utilize voltage controlled inverters are modeled as constant P|V| sources. In each case, the efficiency, η , of the PCU is considered constant and the output power of the PHV system P_G^{DC} , is scaled according to (4.2):

$$P_G^{DC} = \eta \cdot P_G^{DC} \quad (4.2)$$

The constant PQ and constant P|V| power flow component models are described in the following sections.

4.1.1. The Constant PQ Source Model

Most residential and small commercial (<10kW) PHV generators employ inverters which utilize the current control scheme. In this scheme the phase of the current to be output by the PCU is controlled to match a voltage reference measured at the output bus of the inverter. This emphasis on matching the current phase angle to the output bus ensures a high output power factor for the PHV generator [14]. Most commercially available PCU's specify an output power factor close to 1 under normal conditions and no lower than 0.9 [33]. The generator acts as a current source and does not control the voltage at its output bus. Thus a constant PQ model is selected for integration with the power flow module. For this model the real and reactive power injections P_G^{inj} and

Q_G^{inj} are functions of the PHV array model under the given environmental conditions and the assumed PF of the inverter as follows:

$$\begin{aligned} P_G^{inj} &= pf \cdot P_G^{DC} \\ Q_G^{inj} &= (\sin(\arccos(pf))) \cdot P_G^{DC} \\ S_G^{inj} &= P_G^{inj} + jQ_G^{inj} \end{aligned} \quad (4.3)$$

4.1.2. The Constant P|V| Source Model

It is likely that large, three-phase commercial sized (>10kW) PHV generators would incorporate an inverter using the voltage control scheme and thus would act as a voltage source. As such, commercial sized PHV installations will be modeled utilizing a constant P|V| generator model.

For a given environmental condition the apparent power capacity of the generator S_G^{inj} is determined by the PHV array model (4.4) and the desired $|V|$ is specified:

$$|S_G^{inj}| \leq P_G^{DC} \quad (4.5)$$

The current capacity of the PHV generator is limited by S_G^{inj} therefore it is necessary to define another parameter in order to determine the constant P_G^{inj} injection and the reactive power limit $Q_{G,\text{lim}}^{inj}$. In this case, it is appropriate to define a minimum power factor for the power output of the array in order to accomplish this. A power factor of 0.9 will be selected as the minimum power factor because this is stated to be the minimum power factor for some commercially available PCU's [33]. Therefore P_G^{inj} and $Q_{G,\text{lim}}^{inj}$ are calculated in (4.6):

$$\begin{aligned}
P_G^{inj} &= 0.9 \cdot P_G^{DC} \\
Q_{G,\text{lim}}^{inj} &= (\sin(\arccos(0.9))) \cdot P_G^{DC} \\
\text{constraint:} \\
Q_G^{inj} &\leq Q_{G,\text{lim}}^{inj}
\end{aligned} \tag{4.6}$$

The P|V| generator is then integrated with the power flow module in the standard manner a generator bus treated in the Newton Raphson power flow method. When an iteration is completed a value for Q_G^{inj} is calculated and compared to $Q_{G,\text{lim}}^{inj}$. If the constraint is violated the power flow is considered invalid because a solution does not exist where both the constraint and the voltage magnitude requirement are satisfied.

4.2 Power Flow Integration

An unbalanced three phase distribution power flow solver has been developed in [14] and implemented in MATLAB. This implementation models the steady state behavior of a three phase distribution system based on information in a case file which describes the components and topology of the distribution system to be modeled. The power flow model does include an implementation of PQ and P|V| sources.

The power flow models single phase and two phase networks, as well as unbalanced loads and generators. In this implementation load busses often represent aggregate loads such as a pole top transformer which services a number of residential and commercial units, or an industrial substation feeding large industrial loads. The PHV generator model is represented as an injection at the load bus therefore the PHV generator model is also an aggregate of all the PHV generators connected to the given bus. An unbalanced PHV generator may represent a situation where the number and capacity of PHV generators connected to a given bus is unbalanced. In general, large PHV

generators (10>kW) and those modeled as constant P|V| sources are balanced three phase systems and are modeled as such in simulations.

4.2.1. PQ Source Model Integration

As stated in Chapter 2, a PQ source is integrated with the power flow by adding the generated power to the load injected power at bus k as in (4.4):

$$S_k^{inj} = S_{Lk}^{inj} + S_{Gk}^{AC} \quad (4.4)$$

where:

S_k^{inj} = total power injected at bus k

S_{Lk}^{inj} = power injected by the load at bus k

4.2.2. P|V| Source Model Integration

The power injection of the PHV generator must also be combined with the load injection for the constant P|V| case. The real power injection and reactive constraint at bus k are thus defined in (4.5) and the voltage magnitude $|V_k|$ is specified:

$$\begin{aligned} P_k^{inj} &= P_{Lk}^{inj} + P_{Gk}^{inj} \\ Q_{Gk}^{inj} &= Q_k^{inj} - Q_{Lk}^{inj} \\ \text{constraint:} \\ Q_{Gk}^{inj} &\leq Q_{Gk,lim}^{inj} \end{aligned} \quad (4.5)$$

where:

P_{Lk}^{inj} = total real power injection specified for bus k

Q_k^{inj} = total reactive power injection at bus k

calculated from results of the power flow

$(P_{Gk}^{inj}, Q_{Gk}^{inj})$ = real and reactive power injections due to PHV generator

For the Newton Raphson implementation presented in [35] the variable, Jacobian, and mismatch matrices are created based on the network topology before all P|V| busses are determined. Therefore it is necessary to remove the appropriate rows and columns corresponding to the voltage magnitude of P|V| busses. If the constraint is violated the PHV generator model is converted to the constant PQ type with a given power factor, for example 0.9. In this case, the voltage requirement $|V_k|$ will not be met in the solution.

The PHV array and PCU models have been developed and integrated with existing unbalanced distribution power flows. The following chapter presents the implementation details, simulation results and subsequent analysis performed on large scale distribution systems. A 394 bus test system is used as an example

5. Simulation Methods and Results

The model described in Chapters 3 and 4 has been implemented in MATLAB and integrated with an existing power flow program in order to perform system studies on large scale distribution systems. For each power flow computation, a load level and set of environmental conditions must be selected and input to the system. Then, a 394 bus test system of a real world power network is used as an example for the following studies.

5.1. Test System and Case File Construction

The 394 bus test system with 199 load busses that is used for simulation studies in this work is shown in Figure 5.1. For a simulation to be performed a case file must be constructed which describes the system conditions. The case file must contain data for both the electrical and weather conditions in order to fully describe the test system. Electrical data includes load data as well as the location and ratings of installed PHV generators. This section describes the construction of case files which include this information. Cases studies and corresponding result are summarized in Table 5.1

Table 5.1: Summary of simulation study conditions

Example Studies	Study Conditions					Results
	Network Parameters and Configuration	Load Levels	Locations of PHV Systems	Ratings of PHV	Environmental Conditions	
Single Flow	Constant	Constant	Constant	Varied	Constant	Table 1
Twenty Four Hour	Constant	Varied	Constant	Constant for each 24 hour trial	Varied	Figures 5.2, 5.3, 5.4, 5.5

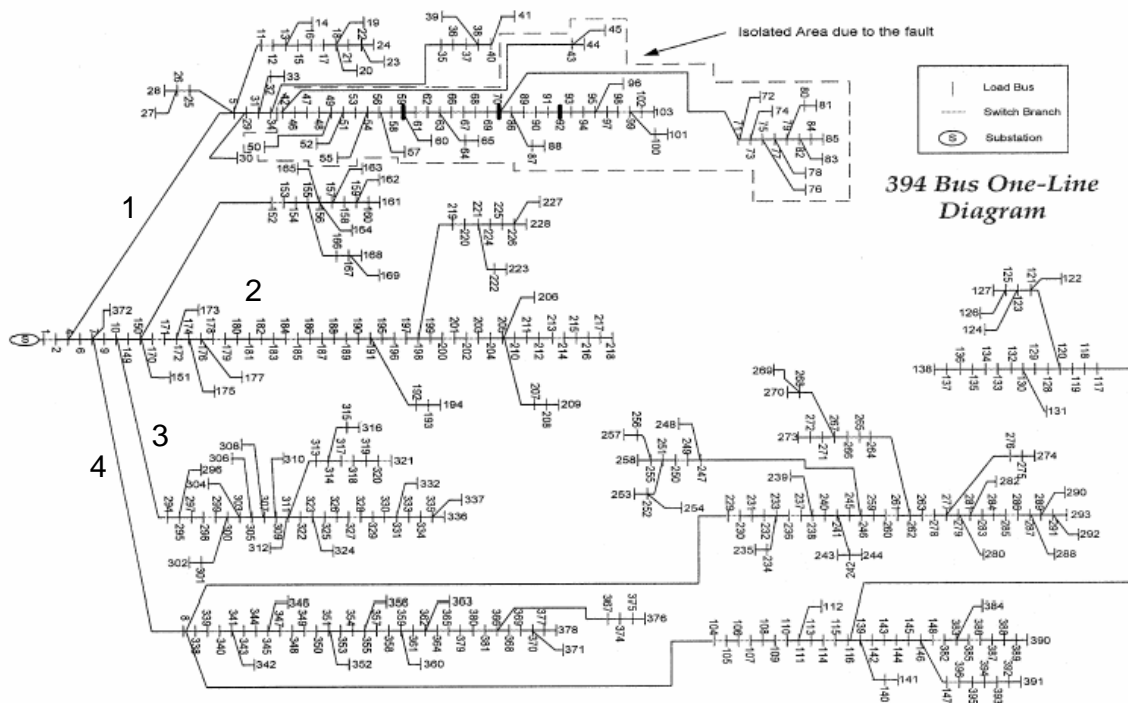


Figure 5.1: One line diagram of 394 bus test system

5.1.1. Electrical System Data

Power flow data includes network, load and generation parameters. This section will focus on the two most relevant components to this work which are the loading conditions and the configuration of installed PHV generators. These will now be discussed respectively.

A base case loading condition was provided for the 394 bus test system, which represented peak demand. The loads have been divided into categories of residential, commercial, and industrial loads and each type of load may be scaled separately to describe a desired loading level.

In order to create 24 hour load profiles from the base case, existing load profiles may be used to describe demand of the test system for a specific hour of a given load profile. Seasonal load profiles are available online for free from Itron through their

eShapes database [15]. This database contains load profiles for ten geographic regions for the years 2001-2005, and specifies the type of load which allows for the use of residential, commercial and industrial example load profiles. These profiles are used to construct load data for case files according to the procedure described in Appendix C.

With respect to PHV generators, the case file must include data on the location and rating of the generator. The 394 bus test system has 199 load buses. It is appropriate to place PHV generators on these busses because of the previously stated trend that most PHV generators are owned by the consumer and placed at the load site. It is also appropriate to place residential sized (<10kW) systems on load busses classified as residential and larger systems on commercial or industrial load busses. Simulation studies will use specific schemes to determine the desired locations and capacity for PHV generators. These schemes will be described in the following sections which outline the specific simulations performed.

5.1.2. Environmental Data

Measured hourly environmental data is available through the Typical Meteorological Year 2 (TMY2) database compiled by the National Renewable Energy Laboratory [27]. This database is a compilation of data measured during the years 1961-1990. It was constructed by selecting months considered to be average months from individual years and concatenating them to form a single year of data. The database was compiled specifically for use in computer simulations of solar energy systems.

The PHV generator model uses two parameters which are available in the TMY2 database, solar irradiation and ambient temperature. Several measurements of irradiance are included in the TMY2 measured data, however the most appropriate for use is that

labeled in [27] as the Global Horizontal Radiation (W/m^2), defined as the total direct and diffuse radiation incident upon a horizontal surface. The array of most solar generators is installed at an angle which maximizes the time at which direct rays from the sun are normal to the surface of the panels. Therefore use of the irradiance measured on a horizontal surface as an input will create a bias which underestimates the production capability of a PHV generator. The measurements which are given

The following sections describe specific simulations and their results. In each simulation environmental data is matched with appropriate load data from the correct season.

5.2. Single Flow Studies

Single power flow studies are the basic tool to be used in building 24 hour or longer studies. Thus given a single set of PHV installation locations and ratings, environmental conditions, network load conditions and network parameters, a power flow study can be made. Here, arbitrary levels of PHV penetration are considered based on a percentage of the total substation demand (real power) of the base case (no PHV generation). Some US state mandates have set a goal of 20% renewable generation and therefore increments of 5% up to 20% have been performed. In each case the total PHV generation was spread evenly over 65 of the 199 load busses. This resulted in PQ bus power flow models of the PHV generators. An arbitrary unbalanced, aggregate PHV installation at each bus was selected with:

- phase A and phase B at 40% of the PHV generation
- phase C at 20%

For this study the peak load levels of the original distribution system case file are used.

In order to measure the level of imbalance at the substation, the percentage difference between the individual phase apparent powers is determined with respect to the total apparent power, $|S_{3\phi}|$, at the substation. For example, between phase a and b , the difference is calculated by the following:

$$|S_{a-b}| \% = \frac{abs(|S_a| - |S_b|)}{(|S_{3\phi}|/3)} * 100 \quad (5.6)$$

The per unit difference in voltage between two phases is calculated as:

$$|V_{a-b}|_{p.u.} = abs(|V_a| - |V_b|) \quad (5.7)$$

The results of the power flow at peak loads for this study are shown in Table 1.

Table 5.2: Imbalance study varying PHV penetration

PHV Penetration	max S _{x-y} %	S _{x-y}	max V _{x-y}	V _{x-y}
0%	3.12	a-b	0.00094	c-a
5%	3.63	c-a	0.00139	b-c
10%	6.50	c-a	0.00178	b-c
20%	8.42	c-a	0.00217	b-c

5.3. Twenty Four Hour Simulation Studies

Twenty four hour simulations are designed to investigate the impacts the intermittent nature of PHV generation has on the distribution system. These simulations use the methods described in section 5.1 to create load profiles which are then matched with an appropriate environmental profile in order to simulate the behavior of a distribution system over the course of a 24 hour period. The environmental data provided are single measurements taken once an hour. Therefore the simulation results are limited

in their ability to model system behavior for the entire 24 hour period. The results do not represent an average of the system behavior over time they represent the system behavior at 24 moments during a 24 hour period.

5.3.1 Example Twenty Four Hour Simulation Study

An example is provided here which studies the behavior of the 394 bus test system on a peak load day with peak irradiance conditions. The example is similar to that of the single flow study presented above in that the total PHV generation was spread evenly over 65 of the 199 load busses, which results in PQ bus power flow models. Again the arbitrary unbalanced, aggregate PHV installation at each bus was selected with:

- phase A and phase B at 40% of the PHV generation
- phase C at 20%

For these simulations loads were categorized and scaled appropriately according to the procedure described above. The base case which contains no PHV generators and thus describes the load profile of the distribution system at the substation is shown in Figure 5.2.

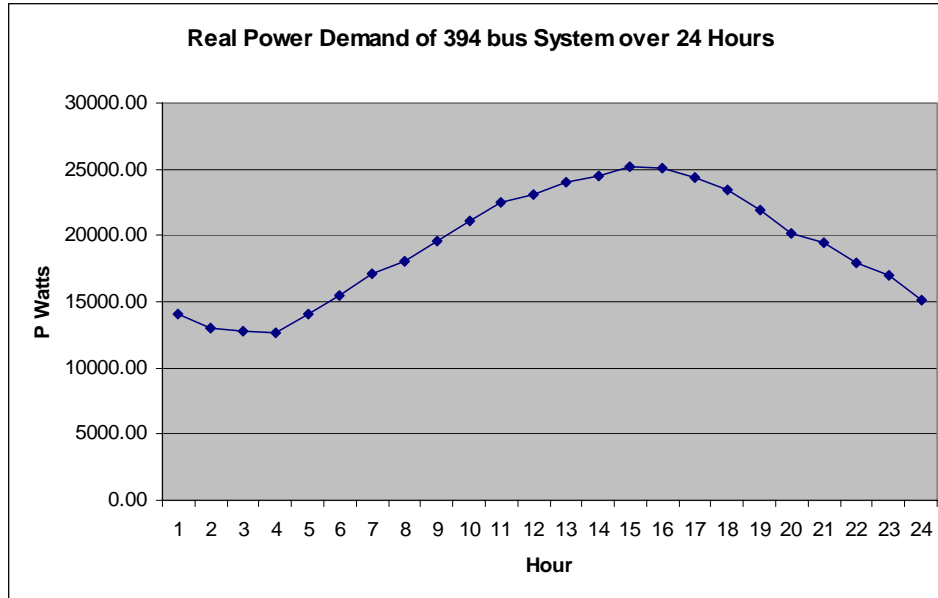


Figure 5.2: Real power demand of the 394 bus test case for peak load

Environmental data corresponding to Binghamton, NY was selected because of its geographical proximity to the 394 bus test system located in Elmira, NY. The day containing the highest irradiance measurement in the TMY2 database was selected for the environmental input as an appropriate pairing for the peak loading day of the distribution system. The corresponding irradiance and temperature curves are shown in Figures 5.3 and 5.4 respectively.

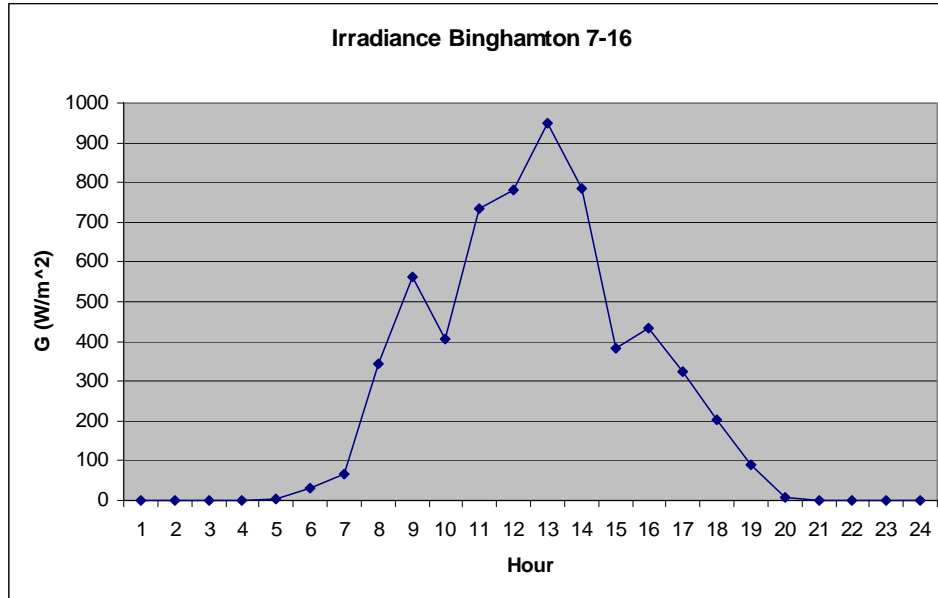


Figure 5.3: TMY2 Irradiance profile for Binghamton NY, July 16

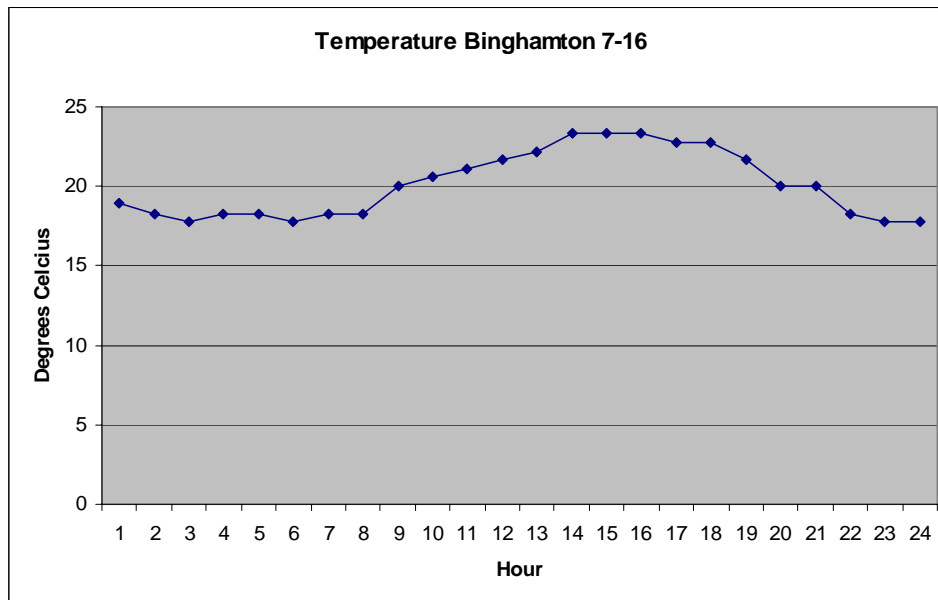


Figure 5.4: TMY2 Ambient temperature profile for Binghamton NY, July 16

The results of the 24 hour simulations are shown in Figure 5.5. As in the single flow simulation the overall rated capacity of installed PHV generation is varied from 5% to 20% of the overall power demand.

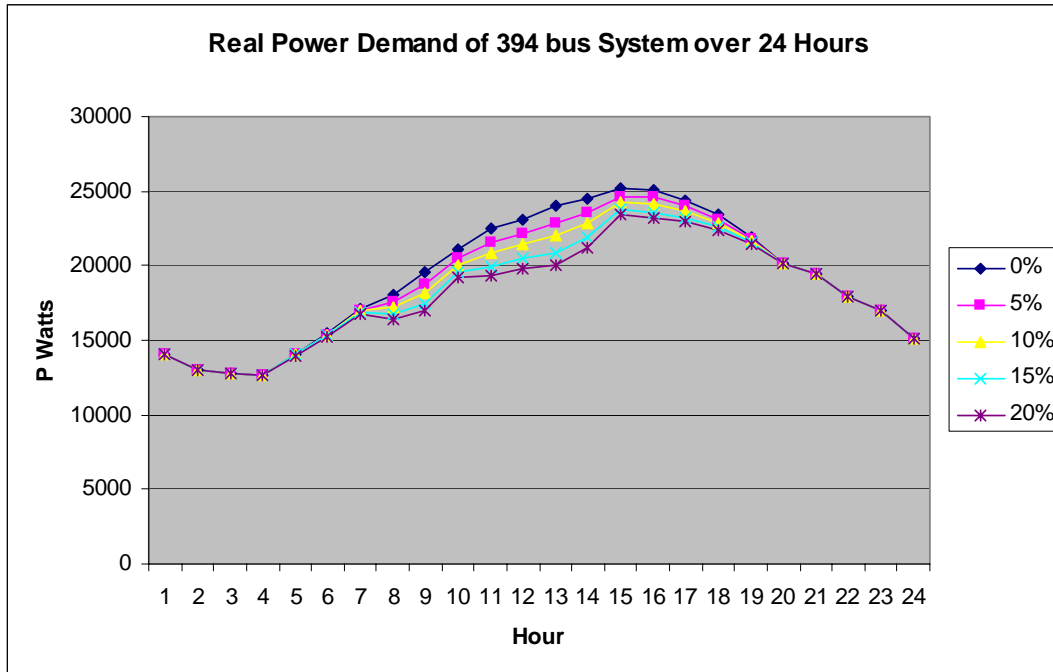


Figure 5.5: Real power demand at the substation under varying capacity of PHV generation

5.3.2. Observations and Remarks

In order to gain insight regarding the nature of PHV generation it is valuable to simulate the power output of an example PHV generator over a 24 hour period using an available environmental profile. Figure 5.6 shows the power output of a 1000W PHV generator under the same environmental conditions used in the previous section (Binghamton NY, 7-16) [27].

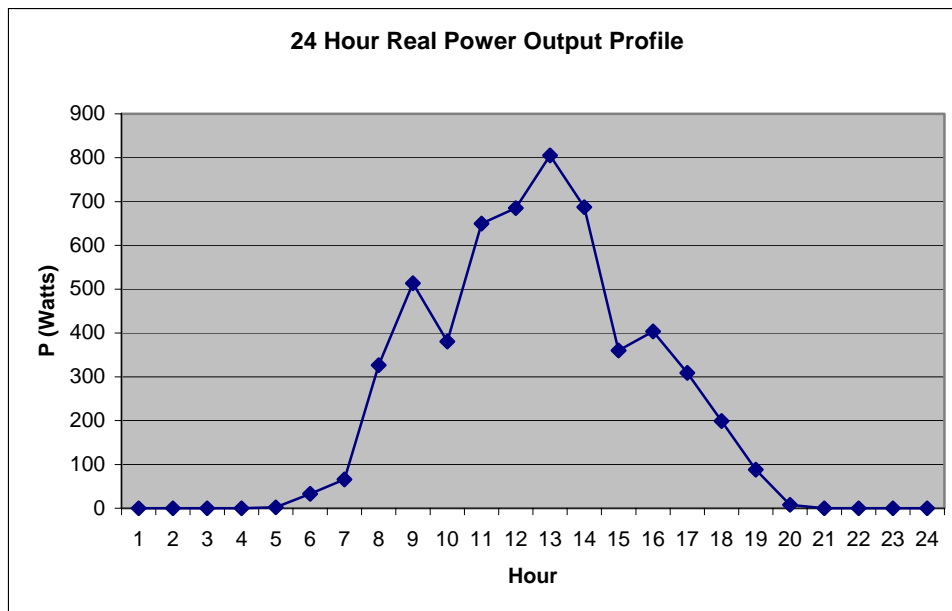


Figure 5.7: Real power output of a 1000W rated PHV generator

By comparing Figure 5.6 to Figures 5.3 and 5.4 it can be seen that the power output of a PHV generator is most heavily impacted by the irradiance incident upon its surface. This conclusion is in agreement with Chapter 3 which states that the electrical energy output of a PHV generator is most directly proportional to the energy input in the form of solar irradiance incident on the surface of the solar array.

Figures 5.3 and 5.5 show one of the potential impacts a high penetration of PHV generation may have on distribution systems. Solar irradiance and thus PHV generator production peaks at 1:00pm followed by a sharp drop off while the load demand peaks at 3:00pm and drops off more slowly towards the end of the day. Therefore overall system demand changes rapidly during this afternoon drop off in solar radiation. This change in load profile could present a new challenge for distribution system planners and operators.

6. Conclusion and Future Work

6.1. Conclusions

This thesis provided a review of PHV generators and presented the development of a mathematical model of a grid connected PHV generator practical for use in large scale distribution systems studies. The model was implemented and integrated with an existing unbalanced distribution system power flow analysis. Simulations were performed using a 394 bus test system with the purpose of identifying and characterizing distribution system impacts of grid connected PHV generators.

The presented PHV generator model was designed specifically for distribution system studies. Therefore, environmental and generator input parameters were limited to those readily available to distribution system planners and operators. The PHV generator model was created using the generally accepted I-V characteristic equation of a PHV cell as its basic building block. The model accounted for the two most common inverter control schemes by allowing for integration with distribution power flow as either a constant PQ or constant P|V| source. The model can be integrated with several methods of distribution power flow and specific schemes for integration with the Newton Raphson, and backward/forward sweep methods were described.

The model was implemented in MATLAB using an existing Newton Raphson unbalanced distribution power flow solver. Simulation methods were developed to capture the intermittent nature of PHV generation. Hourly load levels were calculated using test system peak load levels and publicly available distribution load profiles. These methods were then used along with hourly environmental data to develop case files for 24 hour simulation of distribution systems with installed PHV generation. Simulations were

performed with a 394 bus test system using both single flow and 24 hour simulation methods in order to investigate distribution system impacts of grid connected PHV generation. Specifically phase balancing, feeder balancing, system demand profiles, and voltage rise were addressed.

6.2. Summary of Research Contributions

The work presented in this thesis is a continuation of research in the field of steady state distribution system modeling. The following contributions to this research field have been made:

- Practical PHV generator model for systems engineers requiring limited input data
- Matlab based simulation tool which integrates the PHV model with an unbalanced distribution power flow solver for system studies
- Simulation methods, results, and analysis for 24 hour system studies using a 394 bus test case.
- Demonstrated that increased penetration of single phase PHV generators may increase distribution system imbalance levels which would be a cause of concern for system planners and operators.
- Demonstrated that a 20% penetration of PHV generation will cause significant changes to the shape of daily load profiles.
- Identification of early afternoon (12:00pm-2:00pm) as a time period of concern due to rising demand and sharply decreasing PHV power production.

This thesis provides an additional component model which increases the breadth of cases available for steady state distribution system studies, including an example of its implementation and simulation results.

6.3. Future Work

This thesis can be seen as a first step towards the comprehensive study of grid connected PHV generation, its system impacts and possible control schemes to enhance reliability, power quality, and economic operation of distribution systems. As penetration levels of grid connected PHV generators increase the behavior of distribution systems will become increasingly impacted by the intermittent nature, and single phase characteristics of this renewable energy source. It may be necessary for new schemes to be developed for applications such as load balancing, capacitor placement and switching, service restoration, and distribution automation for economic operation. This work provides engineers with a model which can be used to perform the system studies for investigations into these fields.

This model could be used as a predictive tool where predictions of load and environmental data could be used to predict the steady state behavior of a given distribution system with grid connected PHV generation. Such an application would require additional investigation regarding the PHV model in order to assure the model accurately predicts the behavior of a physical system within a certain margin of error. Such investigations are problematic because they would require a physical PHV generator of the appropriate power rating, as well as the instrumentation necessary to measure environmental inputs and system conditions. The cost of a residential sized PHV generator is on the order of \$10,000 and proper installation requires an appropriate space with unobstructed southern exposure that is also accessible for measurement.

The model presented in this thesis can be utilized in a multitude of studies and investigations. It provides engineers with a steady state simulation engine for distribution

system studies with grid connected PHV generation. It can be used to simulate and analyze distribution systems with varied PHV connection schemes and varied levels of installed PHV capacity only a few of which are included in this work. It can also be used to test and optimize control schemes designed for the case of distribution systems with grid connected PHV generation. This work presents only a sample of the applications for which this model may be used to improve planning and operations for distribution systems with grid connected PHV generation.

References

- [1] K. Aoki, T. Ichimori and M. Kanezashi, "An efficient algorithm for load balancing of transformers and feeders by switch operation in large scale distribution systems," *IEEE Trans. Power Del.*, vol. 3, pp. 1865–1872, Oct. 1988. 1988.
- [2] Austin Energy, "Solar Rebate Program," <http://austinenergy.com/Energy%20Efficiency/Programs/Rebates/Solar%20Rebates/index.htm>. 2006.
- [3] M. E. Baran and F. F. Wu, "Network reconfiguration in distribution system for loss reduction and load balancing," *IEEE Trans. Power Del.*, vol. 4, pp. 1401–1407, Apr. 1989. 1989.
- [4] California Public Utilities Commission, "California Solar Incentive Program," <http://www.cpuc.ca.gov/static/Energy/solar/index.htm>. 2006.
- [5] L. Castaner and S. Silvestre, *Modeling Photovoltaic Systems using PSpice*. West Sussex, England: Wiley, 2002,
- [6] T. -. Chen, M. -. Chen, T. Inoue, P. Kotas and E. A. Chebli, "Three-phase cogenerator and transformer models for distribution system analysis," *IEEE Trans. on Power Delivery*, vol. 6, pp. 1671 - 1681, Oct. 1991. 1991.
- [7] H. Chihchiang and S. Chihming, "Study of maximum power tracking techniques and control of DC/DC converters for photovoltaic power system," *Power Electronics Specialists Conference, 1998. PESC 98 Record. 29th Annual IEEE*, vol. 1, pp. 86, May 17-22. 1998.
- [8] Y. C. Chuang, Y. L. Ke, C. S. Chen and Y. L. Chen, "Distribution system temperature adaptive load transfer using colored petri net approach," *IEEE Trans. on Power Systems*, vol. 8, pp. 2931, Aug. 2006. 2006.
- [9] Energy Information Administration, "State Renewable Energy Requirements and Goals: Status Through 2003," <http://www.eia.doe.gov/oiaf/analysispaper/rps/index.html>. 2004.
- [10] Go Solar Company, "Shell Solar Panes SQ Series," <http://www.solarexpert.com/Shell/Shell-SQ.html>. 2006.

- [11] J. Grainger and W. Stevenson, *Power System Analysis*. New York: McGraw-Hill, 1994, pp. 787.
- [12] F. Groppi, "Grid-connected photovoltaic power systems: Power value and capacity value of PV systems," International Energy Agency, Milano, Italy, Tech. Rep. IEA PVPS T5-11: 2002, February, 2002.
- [13] T. Hoff and D. S. Shugar, "Value of grid-support photovoltaic's in reducing distribution system losses," *IEEE Trans. on Energy Conversion*, vol. 10, Sept. 1995. 1995.
- [14] T. Ishikawa, "Grid-connected photovoltaic power systems: Survey of inverter and related protection equipments," International Energy Agency (IEA), Tokyo Japan, Tech. Rep. IEA-PVPS T5-05: 2002, December, 2002.
- [15] Itron, "eShapes,"
http://www.itron.com/pages/products_detail.asp?id=itr_000491.xml. 2006.
- [16] S. B. Kjaer, J. K. Pedersen and F. Blaabjerg, "A review of single-phase grid-connected inverters for photovoltaic modules," *Industry Applications, IEEE Transactions on*, vol. 41, pp. 1292, Sept.-Oct. 2005.
- [17] F. Ma and D. Curtice, "Distribution Planning and Operations with Intermittent Power Production," *Ieee Transactions on Power Apparatus and Systems*, vol. 8, pp. 2931, August. 1982.
- [18] F. Ma and L. Isaken, "Impact of Dispersed Supply Management on Electric Distribution Planning and Operations," *IEEE Transactions on Power Apparatus and Systems*, vol. 5, pp. 1531, Sept/Oct. 1979.
- [19] A. Makinen, M. Parkki, P. Jarventausta, M. Kortessluoma, P. Verho, S. Vehvilainen, R. Seesvuori and A. Rinta-Opas, "Power quality monitoring as integrated with distribution automation," *Electricity Distribution, 2001. Part 1: Contributions. CIRED. 16th Int. Conf. and Exhibition on (IEE Conf. Publ no. 482)*, vol. 2, pp. 5, 18-21 June 2001. 2001.
- [20] T. Markvart, *Solar Electricity*. Chichester, England: John Wiley & Sons, 1994,
- [21] R. Messenger and J. Ventre, *Photovoltaic Systems Engineering*. USA: CRC Press, 2004,

- [22] K. N. Miu and H. D. Chiang, "Service restoration for unbalanced radial distribution systems with varying loads: solution algorithm," *IEEE Pwr. Eng. Soc. Summer Meeting*, vol. 1, July 1999. 1999.
- [23] K. N. Miu, H. D. Chiang and G. Darling, "Capacitor placement, replacement and control in large-scale distribution systems by a GA-based two-stage algorithm," *IEEE Trans. on Power Systems*, vol. 12, pp. 1160 - 1166, Aug. 1997. 1997.
- [24] K. N. Miu, H. D. Chiang and R. J. McNulty, "Multi-tier service restoration through network reconfiguration and capacitor control for large-scale radial distribution networks," *IEEE Trans. on Power Systems*, pp. 1001 - 1007, Aug. 2000. 2000.
- [25] K. N. Miu, H. D. Chiang, B. Yuan and G. Darling, "Fast service restoration for large-scale distribution systems with priority customers and constraints," *20th Int. Conf. on Power Industry Computer Applications*, pp. 3-9, 11-16 May 1997. 1997.
- [26] S. Naka, T. Genji and Y. Fukuyama, "Practical equipment models for fast distribution power flow considering interconnection of distributed generators," *IEEE Pwr. Eng. Soc. Summer Meeting*, vol. 2, pp. 1007 - 1012, 15-19 July 2001. 2001.
- [27] National Renewable Energy Laboratory (NREL), "Typical Mean Year 2 Database," http://rredc.nrel.gov/solar/old_data/nsrdb/tmy2/.
- [28] Renewable Resource Data Center, "Solar Radiation Resource Information," 2006, <http://rredc.nrel.gov/solar/>. 2006.
- [29] D. Staszkesy, "Application of distributed intelligence to automatic distribution reconfiguration for reliability improvement," *IEEE Pwr. Eng. Soc. General Meeting*, vol. 3, pp. 2621, 12-16 June 2005. 2005.
- [30] G. N. Tiwari, *Solar Energy Fundamentals, Design, Modelling and Applications*. India: CRC Press, 2002,
- [31] B. Verhoeven, "Utility aspects of grid connected photovoltaic power systems," International Energy Agency, Arnhem, The Netherlands, Tech. Rep. IEA PVPS T5-01:1998, December, 1998.
- [32] J. C. Wang, H. D. Chiang, K. N. Miu and G. Darling, "Capacitor placement and real time control in large-scale unbalanced distribution systems: loss reduction formula,

problem formulation, solution methodology and mathematical justification," *IEEE Trans. on Power Delivery*, vol. 12, pp. 953 - 958, April 1997. 1997.

[33] Xantrex, "Xantrex GT Series Grid Tie Solar Inverters," <http://www.xantrex.com/web/id/172/p/1/pt/23/product.asp>. 2006.

[34] Q. Zhou, D. Shirmohammadi and W. H. E. Liu, "Distribution feeder reconfiguration for operation cost reduction," *IEEE Trans. on Power Systems*, vol. 12, pp. 730 - 735, May 1997. 1997.

[35] R. D. Zimmerman, "Comprehensive Distribution Power Flow: Modeling, Formulation, Solution Algorithms and Analysis," *Doctoral Dissertation*, Cornell University, Jan. 1995.

[36] R. D. Zimmerman and H. D. Chiang, "Fast decoupled power flow for unbalanced radial distribution systems," *IEEE Trans. on Power Systems*, vol. 10, pp. 2045 - 2052, Nov. 1995. 1995.

APPENDIX A: List of Symbols by Section

Section 2.1.1. The Photovoltaic Cell

I_D = dark current (A)

I_o = saturation current of the diode (A)

V_c = cell voltage (V)

$q = 1.6 * 10^{-19}$ (coul)

$k = 1.38 * 10^{-23}$ (j / K)

T_{cK} = Cell Temperature (K)

I_c = cell current (A)

I_l = photo current (A)

G = solar irradiance (W/m²)

TA = ambient temperature (°C)

Section 2.2. Unbalanced Distribution Power Flow

V_{k-1} = steady state voltage at bus k-1

V_k = steady state voltage at bus k

I_k = steady state current flow from bus k-1 to bus k

I_k = steady state current flow from bus k to bus k-1

$I_{(G,C,L)k}$ = steady state current injection at bus k

$S_{(G,C,L)k}$ = steady state power injection at bus k

2.2.2. Constant P|V| Sources

Q_k = specified value of reactive power injection at bus k

P_k = specified real power output of the generator at bus k

V_k^t = calculated voltage value in bus k at iteration t

$V_{fic,k}^t$ = calculated voltage of fictitious node of bus k at iteration t

$X_{fic,k}$ = fictitious branch impedance of bus k

3. Photovoltaic Array Model

P_G^{DC} = calculated real power output of the array at given conditions (W)

P_{ra} = rated DC power output of the array (W)

V_{ocM} = module open circuit voltage (V)

I_{scM} = module short circuit current (A)

(I_{mM}, V_{mM}) = module maximum power point (A, V)

P_{rM} = module rated power output (W)

$NOCT$ = nominal operating cell temperature ($^{\circ}C$)

$\left(\frac{\partial I_{scM}}{\partial T_c} \right), \left(\frac{\partial V_{ocM}}{\partial T_c} \right)$ = temperature coefficients

N_{cs} = number of cells in series in the module

G = solar irradiance (W/m^2)

TA = ambient temperature ($^{\circ}C$)

3.1. Characteristic Equation of the Non-Ideal Photovoltaic Cell

I_c = cell current (A)

I_{sc} = cell short circuit current (A)

I_l = cell photo-current (A)

I_o = saturation current of the diode (A)

V_c = cell voltage (V)

R_s = series resistance

R_{sh} = shunt resistance

$q = 1.6 * 10^{-19}$ (coul)

$k = 1.38 * 10^{-23}$ (j / K)

T_{cK} = Cell Temperature (K)

n = nonideality constant of the diode

Note: $I_l = I_{sc}$

3.2. Conversion of Cell Characteristic Equation to Array Characteristic Equation

I_A = array current (A)

V_A = array voltage (A)

$$I_A = N_p I_c$$

$$I_{scA} = N_p I_{sc}$$

$$V_A = N_s V_c$$

$$V_{ocA} = N_s V_{oc}$$

N_s = number of cells connected in series

N_p = number of cells connected in parallel

I_{scA} = short circuit current of the array (A)

V_{ocA} = open circuit voltage of the array (V)

3.3.1. Determine the Connection Scheme of the Array

$ceil()$ = function that rounds to the next highest integer

V_{DC} = The desired nominal DC voltage (usually 500V)

N_{sM} = Number of modules in series required to achieve V_{DC}

P_{Col} = Power rating of a single string of N_{sM} modules

N_{pM} = number of series strings connected in parallel required to achieve P_{rA}

3.3.3. Solve for parameters of the characteristic array equation

P_{rAwoR} = Denotes power the array would output if $R_{sA} = 0$

(V_{rA}, I_{rA}) = Voltage and current of the array at rated power

FF_0 : Fill Factor of the array without a series resistance

T_c = Cell temperature (°C)

T_{c0} = Cell temp at standard test conditions (usually 25°C)

T_A = Ambient temperature (°C)

$NOCT$ = Nominal Operating Cell Temperature

A_r = Denotes rated (max power point at standard test conditions) value of the array

A_E = Denotes value for the array at given environmental conditions

4. Model of the Power Conditioning Unit and Integration with Power Flow

S_G^{AC} = complex power injection by PHV generator

P_G^{AC} = complex power injection by PHV generator

$Q_{G,lim}^{AC}$ = limit of the reactive power injection by the PHV generator

η = efficiency of the PCU

pf = power factor

4.2.1. PQ Source Model Integration

S_k^{inj} = total power injected at bus k

S_{Lk}^{inj} = power injected by the load at bus k

APPENDIX B: Derivation of V_{ocAE}

It will now be shown how equation (3.19) has been developed. Given the I-V

characteristic equation of the solar array at standard test conditions (1000 W/m², 25°C):

$$I_{Ar} = I_{scAr} - N_p I_0 \left(e^{\frac{(V_{Ar} + I_{Ar} R_{sA})q}{nN_s k T_c K}} - 1 \right) \quad (\text{B.1})$$

Set the current to zero in order solve for the open circuit voltage:

$$0 = I_{scAr} - N_p I_0 \left(e^{\frac{V_{ocAr} q}{nN_s k T_c K}} - 1 \right) \quad (\text{B.2})$$

$$V_{ocAr} = \frac{kT_c K}{q} \ln \left(1 + \frac{I_{scAr}}{I_0} \right) \quad (\text{B.3})$$

Now the empirically determined temperature constant is inserted in equation (B.3):

$$V_{ocAr} + \left(\frac{\partial V_{ocA}}{\partial T_c} \right) (T_c - T_{c0}) = \frac{kT_c K}{q} \ln \left(1 + \frac{I_{scAr}}{I_0} \right) \quad (\text{B.4})$$

$$\left(\frac{\partial V_{ocA}}{\partial T_c} \right) (T_c - T_{c0}) = \frac{kT_c K}{q} \ln \left(1 + \frac{I_{scAr}}{I_0} \right) - V_{ocAr} + V_{ocAE} - V_{ocAE} \quad (\text{B.5})$$

Similar to equation 6.

$$V_{ocAE} = \frac{kT_c K}{q} \ln \left(1 + \frac{I_{scAE}}{I_0} \right) \quad (\text{B.6})$$

Substitute for V_{ocAr} and one occurrence of V_{ocAE} :

$$V_{ocAE} = V_{ocAr} + \left(\frac{\partial V_{ocA}}{\partial T_c} \right) (T_c - T_{c0}) + \frac{kT_{cK}}{q} \ln \left(1 + \frac{I_{scAE}}{I_o} \right) - \frac{kT_{cK}}{q} \ln \left(1 + \frac{I_{scAr}}{I_o} \right) \quad (\text{B.7})$$

Using logarithm rules:

$$V_{ocAE} = V_{ocAr} + \left(\frac{\partial V_{ocA}}{\partial T_c} \right) (T_c - T_{c0}) + \frac{kT_{cK}}{q} \ln \left(\frac{1 + \frac{I_{scAE}}{I_o}}{1 + \frac{I_{scAr}}{I_o}} \right) \quad (\text{B.8})$$

In general unity can be neglected in the numerator and denominator of the log term in equation 11 and thus it reduces to:

$$V_{ocAE} \approx V_{ocAr} + \left(\frac{\partial V_{ocA}}{\partial T_c} \right) (T_c - T_{c0}) + \frac{kT_{cK}}{q} \ln \left(\frac{I_{scAE}}{I_{scAr}} \right) \quad (\text{B.9})$$

APPENDIX C: Calculating the Load Level for a Given Power Flow

In the case file load data is included for each load bus at conditions of peak demand. Many combinations are possible for the type of load and model used. Balanced or unbalanced, and grounded or ungrounded load types are possible and each load can be modeled using the constant power, constant impedance or constant current load models. Regardless of the model used however the load data which is input to the model is in the form of power consumption at the given bus (C.1):

$$\left(S_{P,k}^A, S_{P,k}^B, S_{P,k}^C \right) \quad (C.1)$$

where:

$$S_{P,k}^A = \text{peak power consumption on phase A of bus k (kVA)}$$

In order to model the behavior of a distribution system for a specific situation such as a given hour of a given day of the year it is necessary to scale this peak load in an appropriate manner to describe the situation which is desired for test. Load scalars are defined in order to perform this function. Because different types of loads exhibit different loading profiles three types of loads are considered separately, these are industrial, commercial and residential loads. Scalars are calculated for each type of load in order to model the load behavior of the entire system more accurately. Two scalars are used to calculate the load level for a specific hour of a specific day of the year. The first scalar Sd_d referred to as the day scalar is used to calculate the peak load on a given day (C.2):

$$|S_{Pd,k}| = |S_{P,k}| \cdot |Sd_d^{(I,C,R)}| \quad (C.2)$$

where:

Sd_d = day scalar for day d

(I,C,R) = denotes (industrial, commercial, residential) load type

$S_{Pd,k}$ = peak power consumption on day d on bus k (kVA)

The parameter Sd_d is calculated from a given set of loading data. It is not necessary for the load data to be specific to the distribution system under test, it is only necessary that the load data be from a distribution system load of the same type (I,C,R) . Sd_d is calculated as follows:

$$Sd_d = \frac{|Sl_{Pd}|}{|Sl_p|} \quad (C.3)$$

where:

Sl_{Pd} = peak load on day d from given load data

Sl_p = peak load for the entire year from given load data

Once the peak load on a given day is determined the load for any hour of that day can be calculated using the scalar $Sh_{d,h}$ referred to as the hour scalar, as follows:

$$|S_{d,h,k}| = |S_{Pd,k}| \cdot |Sh_{d,h}^{(I,C,R)}| \quad (C.4)$$

where:

$Sh_{d,h}$ = hour scalar for day d, hour h

$S_{d,h,k}$ = power consumption on day d, hour h, at bus k

The parameter $Sh_{d,h}$ is calculated from load data on the given day in a similar manner as the day scalar:

$$Sh_{d,h} = \frac{|Sl_{d,h}|}{|Sl_{pd}|} \quad (C.5)$$

where:

$Sl_{d,h}$ = power consumption for day d , hour h , from given load data

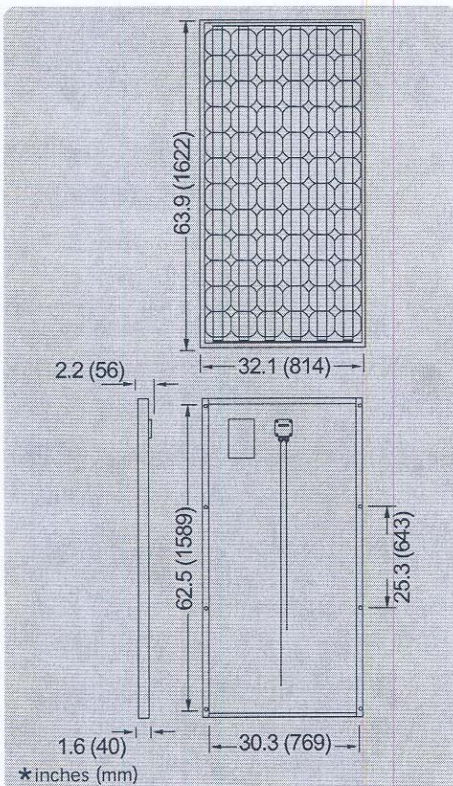
In this manner given the necessary load data the power consumption for all load busses on the 394 bus test system can be determined for any day of the year at any hour of the day. This describes the ideal case where daily load data is available for the period of a year. This specific data is not always available, as often load data is grouped by season where four sets of data are used to describe average days for the four seasons. In this case the calculations above are valid however it would be appropriate for notation purposes to replace the d which denotes day with an s to denote season.

APPENDIX E: EXAMPLE SOLAR MODULE SPEC SHEET

Shell SQ150-PC Photovoltaic Solar Module

Mechanical Specifications Module

A torsion and corrosion-resistant anodized aluminium frame ensures dependable performance, even under harsh weather conditions. Pre-drilled mounting holes are provided for ease of installation.



Outside dimensions (in)	63.9 x 32.1
Thickness (inc. junction box) (in)	2.2
Thickness (exc. junction box) (in)	1.6
Weight (lbs)	38
Cable length - male (in)	51
Cable length + female (in)	39

For installation instructions, please refer to the **Installation Manual** which is available from Shell Solar.

Electrical Characteristics

Data at Standard Test Conditions (STC)

STC: irradiance level 1000W/m², spectrum AM 1.5 and cell temperature 25°C

Rated power	P_r	150W
Peak power*	P_{mpp}^*	150W
Peak power voltage	V_{mpp}	34V
Peak power current	I_{mpp}	4.4A
Open circuit voltage	V_{oc}	43.4V
Short circuit current	I_{sc}	4.8A
Series fuse rating		15A
Minimum peak power	$P_{mpp\ min}$	142.5W
*Tolerance on Peak Power		±5%

The abbreviation 'mpp' stands for Maximum Power Point.

Typical data at Nominal Operating Cell Temperature (NOCT) conditions

NOCT: 800W/m² irradiance level, AM 1.5 spectrum, wind velocity 1m/s, T_{amb} 20°C

Temperature	T_{NOCT}	46°C
Mpp power	P_{mpp}	108W
Mpp voltage	V_{mpp}	31V
Open circuit voltage	V_{oc}	39.6V
Short circuit current	I_{sc}	3.9A

Typical data at low irradiance

The relative reduction of module efficiency at an irradiance of 200W/m² in relation to 1000W/m² both at 25°C cell temperature and AM 1.5 spectrum is 8%.

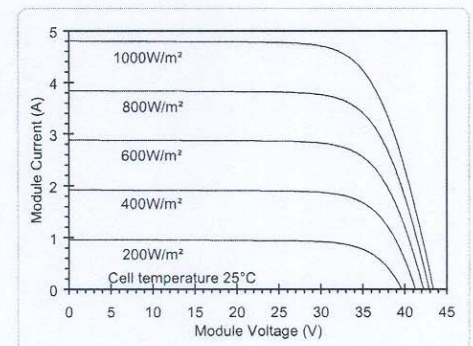
Temperature coefficients

αP_{mpp}	-0.52%/°C
αV_{mpp}	-167mV/°C
αI_{sc}	1.4mA/°C
αV_{oc}	-161mV/°C

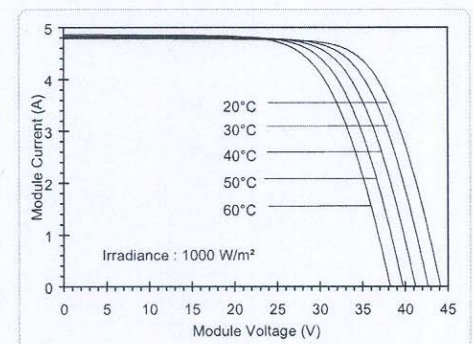
Maximum system voltage: 600 Vdc (UL)

Typical I/V Characteristics

The I/V graph below shows the typical performance of the solar module at various levels of irradiance.



The I/V graph below shows the typical performance of the solar module at various cell temperatures.



References in this Product Information Sheet to 'Shell Solar' are to companies and other organizational entities within the Royal Dutch/Shell Group of Companies that are engaged in the photovoltaic solar energy business. Shell Solar has its principal office in Amsterdam, the Netherlands.

For further information on all Shell Solar products contact:

Shell Solar
4650 Adohr Lane, Camarillo CA 93012
805-482-6800 Fax 805-388-6395
Web www.shell.com/solar

V5/SQ150-PC/02/04/US

